5-8-2019

Fine-scale microclimatic controls on soil carbon dioxide fluxes in a northern hardwood forest

Will Saunders
willib48@gmail.com

FINE-SCALE MICROCLIMATIC CONTROLS ON SOIL CARBON DIOXIDE FLUXES IN A NORTHERN HARDWOOD FOREST

by

Will Saunders

A thesis
submitted in partial fulfillment
of the requirements for the
Master of Science Degree
State University of New York
College of Environmental Science and Forestry Syracuse, New York
May 2019

Department of Forest and Natural Resources Management

Approved by:
Colin Beier, Major Professor
Andrea Feldpausch-Parker, Chair, Examining Committee
Christopher Nowak, Department Chair
S. Scott Shannon, Dean, The Graduate School

ACKNOWLEDGMENTS

This project would not have been possible without the support and encouragement of my major professor, Dr. Colin Beier. I would like to thank him for giving me the chance to work on this project and his guidance throughout my research. His mentorship, knowledge and friendship were an invaluable part of my time at SUNY ESF and I will be forever grateful for his assistance in my pursuits.

I also want to thank my committee members, Dr. John Drake and Dr. Charles Driscoll, for providing their valuable time, advice and direction throughout the project. I would like to especially acknowledge Dr. John Drake who was always willing to help me as I was learning to use and understand the outputs from Project R. I would like to also thank Dr. Eddie Bevilacqua who accepted the role as examiner, and Dr. Andrea Feldpausch-Parker who served as the defense chair.

Further, I would like to thank Pat McHale and L. J. Mills for their extensive help with instrumentation, data collection and support in the field. I owe many thanks to Dr. Timothy Volk, Dr. Lianjun Zhang, Dave Eichorn, Charles Schirmer, Dr. John Stella, and all of the staff at the Adirondack Ecological Center, for their help, accommodations, and guidance in collecting, analyzing, and interpreting data.

None of this would have been possible without the support from my friends and colleagues. Most of all, I want to thank my sister Jackie, for always believing in me and all the support she provided as I pursued my passions, and my girlfriend Vaishnavi, for her unconditional love, support, and for having my back.

Table of Contents

List of Tables

List of Figures

Abstract

W. B. Saunders. Fine-scale microclimatic controls on soil carbon dioxide fluxes in a northern hardwood forest, 96 pages, 13 tables, 20 figures, 2019. APA style guide used.

Carbon dioxide (CO_2) emissions from soil are typically the largest carbon flux from forest ecosystems to the atmosphere, representing a significant biogenic source of greenhouse gases. Although the temperature and moisture sensitivities of the respiration processes underlying soil CO_2 fluxes are well studied, the impacts of a changing climate on these abiotic controls and the resulting soil flux responses are unresolved. Using in-situ continuous measurements of soil microclimate at sites with contrasting hydrology, this study assessed the temperature and moisture dependence of soil CO_2 fluxes within hardwood forests of the Adirondack Mountains in northern New York State (USA). During the 2018 growing season, soil CO_2 fluxes were very strongly coupled with soil temperature and only weakly coupled with soil moisture. Statistical modeling indicated that the relationship between soil moisture and the CO_2 flux was driven by their covariation with soil temperature. Moderate drought conditions during the 2018 growing season affirmed the importance of soil moisture regimes in mediating weather variability, yet there was limited evidence to indicate that respiration was significantly moisture-limited.

Key Words: soil carbon dioxide flux, soil respiration, temperature, soil moisture, climate change, forest soils, northern hardwood forest, Adirondacks, drought

W. B. Saunders
Candidate for the degree of Master of Science, May 2019
Colin Beier, Ph.D.
Department of Forest and Natural Resources Management
State University of New York College of Environmental Science and Forestry
Syracuse, New York

Introduction

The flux of carbon dioxide (CO_2) from soils is a significant component of the global carbon cycle (Raich & Schlesinger, 1992; Schlesinger & Andrews, 2000), but many of the interactions that drive this ecosystem process remain uncertain (Lloyd & Taylor, 1994; Xu et al., 2004; Carey et al., 2016). The soil CO_2 flux is one of the largest carbon ecosystem fluxes (Davidson et al., 1998; Raich et al., 2002; Ryan & Law, 2005; Carey et al., 2016) that incorporates the waste products of respiration by both autotrophs (Ra) and heterotrophs (Rh). Autotrophic respiration in the soil is conducted by plant roots as they metabolize sugars produced via photosynthesis, while heterotrophic respiration results from metabolism of soil-dwelling bacteria, fungi and fauna that conduct organic matter decomposition (Lloyd & Taylor, 1994; Ryan & Law, 2005). Soil respiration rates and the resulting fluxes of CO_2 to the atmosphere, which vary widely across biomes and within a given ecosystem type, are known to be affected by abiotic (e.g., temperature, moisture), biotic (e.g., organic matter content and quality, microbial community composition) and anthropogenic (e.g., land use history) factors (Raich & Schlesinger, 1992; Lloyd & Taylor, 1994; Davidson et al., 1998; Senevirante et al., 2010; Carey et al., 2016). In forests, where the largest pool of carbon is typically soil, changes in soil CO_2 flux can shift these ecosystems from net sinks to sources of carbon, with implications for global carbon cycling and greenhouse gas balance (Schlesinger & Andrews, 2000; Xu et al., 2004; Carey et al., 2016).

The role of the microclimate in exerting fine-scale controls on CO_2 fluxes is important to better understand the potential changes in carbon cycling in forest ecosystems. Temperature has been the most studied abiotic driver of soil respiration, with attention to the influence of

warming soil and air temperatures. Soil respiration is temperature dependent, as biochemical reactions that drive microbial activity and fine root production in soils, rely upon higher rates of respiration to generate the energy needed. Higher temperatures increase reaction rates and soil respiration to a point where soil respiration becomes constrained by higher temperatures, as biological activity declines due to enzyme denaturation and complex temperature regulatory responses in cells. At lower temperatures, soil respiration is limited by slower reaction rates that do not provided enough energy to sustain biological activity. Q_{10}, which is the factor by which the rate of a reaction will increase with every 10-degree increase in temperature, has also been shown to be higher at lower temperatures with declining values as temperature increases (Lloyd & Taylor, 1994; Davidson & Janssens, 2006; Schipper at al., 2014). Although studies consistently find that soil CO_2 flux is positively correlated with temperature (Richey, 1994; Davidson et al., 1998; Liang et al., 2004; Allison & Treseder, 2008; Ullha & Moore, 2011), there have been inconsistent results regarding the rate and the specific nature (e.g., shape of response curve) of this temperature dependent relationship (Lloyd & Taylor, 1994; Xu et al., 2004; Carey et al., 2016).

At high temperatures, the rate of increase in CO_2 flux starts to decline, especially in mesic temperate forests due to moisture limitation (McHale et al., 1998; Carey et al., 2016). Soil moisture and temperature both regulate soil CO_2 flux, with temperature having the greater influence when soil moisture is in an optimal range. Several studies have found soil moisture to be a limiting factor under drought conditions (Davidson et al., 1998; Knapp et al., 2002; Yuste et al., 2003; Xu et al., 2004; C. W. Harper et al., 2005). Low soil moisture can decrease soil respiration due to limited availability of soluble organic C substrates in water films. Soil

microbes and roots are unable to access organic material needed for biochemical reactions, lowering the rate of respiration in the soils. At the other extreme of soil moisture, soils that become highly saturated can impact respiration rates as well as the CO_2 flux, although these effects may be decoupled. Water fills up air pore space in saturated soils, causing anoxic conditions by lowering the diffusion rate of O_2 into the soils. The oxygen needed for aerobic respiration becomes less accessible to soil microbes and roots, lowering soil respiration rates. At the same time, saturated soils can lower the diffusion rate of CO_2 out of the soils, creating a physical barrier that impedes the release of CO_2 via soil pore spaces to the atmosphere. Aerobic respiration could still be occurring deeper in the soil profile, but measurements of soil CO_2 flux would be impeded due to this physical obstruction (Davidson et al., 1998; Davidson et al., 2000; Ryan & Law, 2005). Sites like wetlands that are saturated more often and have more hydric substrates tend to have lower measurable rates of soil respiration under 'normal' conditions (Davidson et al., 1998; Savage & Davidson, 2001; Ryan & Law, 2005; Ullha & Moore, 2011), and this is likely due to both mechanisms (oxygen limitation of aerobic respiration and poor gaseous CO_2 diffusion in saturated pore spaces). For these reasons, identifying when soil moisture becomes a limiting factor is important for accurately modeling soil CO_2 flux.

Numerous studies have been conducted to evaluate the temperature dependency and the soil moisture threshold(s) of soil respiration. At Harvard Forest in central Massachusetts, USA, studies have been measuring soil CO_2 fluxes for over two decades to understand a variety of influences on soil respiration (Giasson et al., 2013). Davidson et al. (1998) measured spatial and temporal associations between soil respiration, moisture, and temperature across soil drainage classes. Soil CO_2 flux was confirmed to be strongly coupled with temperature, with an

exponential model accounting for 80% of the observed variation in the flux. Soil drainage classes also influenced soil CO_2 flux, with lower fluxes observed in wetlands and poorly-drained soils than in mesic and well-drained soils. During the study, a late summer drought resulted in decreases in CO_2 from well-drained soils, while there were simultaneous flux increases from poorly-drained soils. The temperature model predicted soil CO_2 flux well for most the year, but during the drought months, a model incorporating soil moisture along with temperature was needed to explain variation seen in the flux. Drying of well-drained soils likely created limiting conditions for respiration by roots and microbes. In the poorly drained soils, the drought conditions may have allowed for a release of CO_2 that had been impeded by saturated soils, and/or removed the limitation of poor O_2 diffusion, producing more favorable conditions for soil respiration (Davidson et al., 1998). Ullah and Moore (2011) observed a similar phenomenon in a temperate forest in the St. Lawrence River Valley of Canada. Soil drainage characteristics were found to be important when estimating the soil CO_2 flux across the forested landscape. Soil temperature was found to be more important than soil moisture for estimating CO_2 fluxes from well-drained soils, where soil moisture was more important in poorly-drained soils. Based on these findings, soil drainage characteristics related to topographic index need to be considered in order to estimate soil fluxes at a watershed scale (Ullah & Moore, 2011).

The soil microclimate (temperature and soil moisture) are fundamentally shaped by the ambient weather conditions, and several studies have suggested that small changes in local climate will significantly influence rates of soil respiration (Savage & Davidson, 2001; Xu et al., 2004; Senevirante et al., 2010). The interaction between temperature and soil moisture is more variable in temperate ecosystems than tropical (moisture limited) or boreal (temperature

limited) ecosystems, as temperature and moisture regimes vary seasonally and across ecosystems (Senevirante et al., 2010). Determining when soil moisture becomes a limiting factor is more difficult because of this variability and the relationship between the moisture content of soil and its temperature stability. During the Davidson et al. (1998) study, temperature and soil moisture were (negatively) correlated across seasons, with a warm and dry summer and a cool and wet winter. It was impossible to distinguish between the effects of the two factors when there was moderate to high soil moisture. A lower threshold of soil moisture was discovered due to the drought that occurred during the study. Without the occurrence of the drought, the soil moisture threshold may not have been discovered for these sites, leaving temperature as the only consistent predictor of temporal variation in soil CO_2 flux. To identify such thresholds and their effects, flux measurements need to be carefully distributed both temporally and spatially. The drought at Harvard forest was observed due to the temporal duration of the study, while sampling locations were selected to evaluate how topography and soil moisture regimes mediated the effects of ambient weather conditions (Davidson et al., 1998; Ullah & Moore, 2011).

While temperature and soil moisture vary across temperate systems, forest ecosystems effectively regulate their microclimates and can provide more stability for ecosystem processes such as soil respiration. Overstory tree canopies buffer the understory from direct solar radiation, leading to a moderation of higher temperatures during summer months (Fetcher et al., 1985; Chen et al., 1993; K. A. Harper et al., 2005). The alteration of solar radiation leads to higher levels of soil moisture in forest ecosystems due to lower rates of evaporation directly from soils below the canopy, and lesser evaporative demand resulting in lower rates of

evapotranspiration by plants. These effects are evident in forestry studies on gap dynamics and forest fragmentation, where the microclimates of large gaps and clear-cut areas are compared to the edges and understory of intact forest. In the clearings and larger gaps, temperatures rise and fall faster than inside the forest, reaching a higher maximum and lower minimum daily temperature (Fetcher et al., 1985; Chen et al., 1993; Strong et al., 1997; K. A. Harper et al., 2005). Frost was found to occurred more readily in the clear-cut areas, causing damage to sensitive vegetation (de Freitas & Enright, 1995). Temperature and humidity are more stable beneath the closed canopy than in the clearings and gaps, leading to less diurnal variation in the microclimate (Fetcher et al., 1985; Chen et al., 1993).

Recent climatic changes have made the US Northeast region significantly warmer and wetter over the last few decades (Griffiths & Bradley, 2007; DeGaetano, 2009; Brown et al., 2010; Horton et al., 2014; U.S. Global Change Research Program (USGCRP 2018); Howarth et al., 2019). Increases in temperatures across the US Northeast have ranged from approximately 0.6 to 1.7+°C since 1901. Temperatures are predicted to increase by 2.8°C by 2050 under the lower emissions scenario (RCP 4.5), and increase by 2.2°C by 2050 under the higher emissions scenario (RCP 8.5). The US Northeast has also seen the greatest increase (55%) in the amount of precipitation falling in heavy rain events between 1958-2012 among all the US regions (USGCRP, 2018). These high magnitude rainfall events have become more frequent over the last century, with 50-year and 100-year storms occurring at roughly a 40% shorter return interval (DeGaetano, 2009). There has been a statistically significant increase in precipitation attributable to the top 1% precipitation, and in the frequency and magnitude of extreme weather events. The frequency of these top 1% precipitation events increased by 15 events per

year and the annual daily maximum precipitation increased 58.0 mm from 1979–2014, with the most robust trends particularly in September through November (Howarth et al., 2019). There has been an observed decreasing trend in consecutive dry days (CDD) from weather stations in New York (Griffiths & Bradley, 2007; Brown et al., 2010; Insaf et al., 2013; Thibeault & Seth, 2014). However, model forecasts suggest that with increases in the magnitude of rainfall, there may also be decreases in rainfall frequency, leading to overall longer periods of dry weather (CDD) between rainfall events (Sillmann et al., 2013; Singh et al., 2013; Wuebbles et al., 2014). Warming temperatures can lead to earlier snowmelt and increases in the growing season, altering the availability and timing of soil moisture for the ecosystem (Groffman et al., 2001; Horton et al., 2014; USGCRP, 2018). Warmer temperatures are expected to increase evapotranspiration which, if not offset by concomitant increases in precipitation, could exacerbate short term droughts in warmer months (Horton et al., 2014; Wuebbles et al., 2014; USGCRP, 2018). However, it widely known that drought forecasts for New York's future climate are marked with large uncertainty (Horton et al., 2014).

Experimental manipulations in temperate forest have yielded some insights on soil respiration and CO_2 flux response to changes in a warmer climate. McHale et al. (1998) conducted experimental warming of soil temperatures (+2.5, 5.0, 7.5 °C) in an eastern temperate deciduous forest in New York. An increase in the soil CO_2 flux was evident in warmed soils, with the + 2.5°C and + 5.0°C plots having the highest fluxes. It was observed that the + 7.5°C plot did not have the highest flux but was more closely related to the reference plot. These findings could be attributed to a limitation in soil moisture in the warmest plot, as the +7.5°C plot exhibited the lowest soil water tension during the study (McHale et al., 1998).

Groffman et al. (2001) simulated declines in snow pack due to warmer temperatures by experimentally removing snow from plots in Hubbard Brook Experimental Forest, which exposed soils to colder temperatures during early winter. Snow removal led to mild soil freezing events that caused significant increases in fine root mortality and leaching of soil solutes. Changes to the available solutes and increased fine root mortality over winter could influence soil respiration rates (and CO_2 fluxes) during the early growing season and potentially decrease net productivity (Groffman et al., 2001).

Changes in the timing, frequency, and intensity of precipitation events may also influence respiration and CO_2 flux, especially in well-drained mesic soils. For example, an increase in the period of dry days between precipitation events could increase the likelihood of soils reaching their wilting point, creating limiting conditions for respiration. After the next rain event remoistens the soil, a brief increase (or pulse) in soil CO_2 flux is a well-documented phenomenon known as the 'Birch effect' (Birch, 1958), which is attributed to favorable conditions for the immediate response of both roots and microbes (Lee et al., 2002; Yuste et al., 2003; Xu et al., 2004; Warren, 2014, 2016). Changes to the normal timing and amount of precipitation has been shown to impact soil respiration over a growing season. Knapp et al. (2002) and C. W. Harper et al. (2005) altered the precipitation regime of a temperate grassland in Kansas to simulate the predicted increases in both intense rainfall and the mean number of dry days between rainfall events, under both ambient and reduced rainfall quantities. Four rainfall regimes were implemented during the study: ambient rainfall quantity and timing, reduced rainfall quantity with ambient timing, altered rainfall timing (increase in dry days) with ambient quantity, and altered timing with reduced quantity. In this experiment, soil CO_2 flux

decreased by 8% under reduced rainfall, decreased by 13% under increased dry periods between rain events, and decreased by 20% under both conditions. The variability in precipitation led to an overall decrease in soil CO_2 flux and belowground productivity throughout the growing season (Knapp et al, 2002; C. W. Harper et al., 2005).

The interactions between ambient weather conditions, the regulating influence of the forest environment on temperature and moisture, and soil drainage characteristics shape the microclimate of the forest soil, which in turn regulates soil respiration and CO_2 fluxes. These interactions require more detailed investigations (Senevirante et al., 2010; Davidson et al., 2012; Carey et al., 2016) to explain spatial and temporal variation in observed soil CO_2 fluxes and their potential responses under changing climate conditions. Understanding these interacting controls on soil respiration is essential to accurate forecasting of climate-induced changes in forest carbon cycling (Davidson et al., 1998; Schlesinger & Andrews, 2000; Carey et al., 2016). Temperature increases are expected to increase soil CO_2 flux, decreasing the soil carbon stock and increasing atmospheric CO_2, if all factors are held equal (Raich & Schlesinger, 1992; Schlesinger & Andrews, 2000), but several studies have found a neutral or negative response to warming, due to moisture limitations, shifts in physiological response and/or depletion of labile C pools (Carey et al., 2016). If increases in precipitation cannot keep pace with increases in evapotranspiration due to higher temperatures, more frequent short-term droughts could occur. Increases in extreme precipitation could lead to more saturating events in mesic soils (Senevirante et al., 2010; Horton et al., 2014; Wuebbles et al., 2014; USGCRP, 2018; Howarth et al., 2019). Because both types of moisture extremes can occur in the same growing season, understanding their impact on soil gas fluxes rates poses a complex problem.

Given that climate forecasts for the US Northeast indicate an increasing likelihood of both high and low soil moisture extremes, a better understanding of how soil moisture interacts with temperature controls on soil CO_2 flux in the region's temperate forests is needed for accurate modeling of forest carbon cycling in a changing climate (Schlesinger & Andrews, 2000; Xu et al., 2004; Carey et al., 2016). Creation of an overall global model has been difficult due to site specific parameterization of temperature and soil moisture relationships, and the confounding effects of temperature, soil moisture and environmental drivers (e.g., substrate availability and quality, soil type, plant species composition, etc.) obscuring the individual effects on soil respiration. In other words, the temperature dependency coefficient Q_{10} is strongly influenced by local environmental conditions (Davidson et al., 2006; Davidson & Janssens, 2006; Davidson et al., 2012; Schipper at al., 2014; Carey et al., 2016). Site specific studies continue to be needed to parameterize the relationships between soil gas fluxes and the microclimate within and across ecosystem types. Specifically, in mesic temperate forests, the challenge of estimating the threshold(s) of soil moisture limitation in response to ambient weather conditions requires consideration of spatial heterogeneity in soil moisture regimes (i.e., topography).

In this study, the approach used by Davidson et al. (1998) was generally reproduced to observe the impacts of soil moisture extremes, particularly increases in high-magnitude rain events, on soil CO_2 fluxes in well-drained and poorly-drained soils in the northern hardwood forests of the Adirondack Mountains (New York State, USA).

Objectives

The first objective of this study was to evaluate the relationships between ambient weather conditions and the in-situ soil microclimate. As a rule, the subcanopy microclimate is more stable than that of an open field, with canopy cover moderating temperature maxima and minima (less diurnal variation in temperature) and lowering rates of evapotranspiration (higher soil moisture; Fetcher et al., 1985; Chen et al., 1993). I hypothesized that in-situ measurements of the forest microclimate would more accurately model the soil CO_2 flux as compared to open-field meteorological measurements. I also compared the subcanopy measurements to those from weather stations in open fields to provide a better understanding of how changes in ambient weather conditions were mediated in the subcanopy microclimate. The relationship between the microclimate measurements in open fields and subcanopy was applied to develop rough predictions of future CO_2 flux (based on forecasted warming).

The second objective of this study was the role of the soil microclimate in exerting fine-scale controls on CO_2 fluxes in well-drained and poorly-drained mesic soils. Temperature is a well-known predictor variable of soil CO_2 flux, as respiration is a temperature depend reaction, and soil temperature has lower variation than air temperature above the soils (Richey, 1994; Davidson et al., 1998; Ullha & Moore, 2011). Soil moisture is known to limit both respiration and the measurement of the flux, but when it becomes a limiting factor is still inconclusive (Davidson et al., 1998; Knapp et al., 2002; C. W. Harper et al., 2005). Soil drainage characteristics have also been found to influence the flux, especially in poorly-drained soils and should be accounted for when modeling across forest or watershed scales (Davidson et al., 1998; Ullha & Moore, 2011). To accurately model these relationships, the methodology from

Davidson et al. (1998) and Ullah & Moore (2011) were modified to measure soil CO_2 flux (not teasing apart Ra and Rh) and the microclimate throughout the growing season at a fine spatial scale in two sites with different soil drainage characteristics. Both a well-drained and a poorly-drained mesic soil were used to try to observe both the high and low threshold of soil moisture under varying conditions.

The final objective of this study was the role of extreme soil moisture events in impacting soil CO_2 fluxes, in a northern hardwood forest ecosystem. With the US Northeast experiencing more high magnitude rainfall events, soil could be saturated more often, suppressing the infusion of O_2 or the release of CO_2 (Davidson et al., 1998; Davidson et al., 2000; Ryan & Law, 2005; USGCRP, 2018). I initially set out to look at the effect of soil saturating events on soil CO_2 flux, but ended up capturing one of the driest growing seasons in recent decades. The continuous in-situ microclimate measurements allowed for drying down periods to be observed during the study. Short term droughts are being forecasted for the US Northeast with warmer temperatures predicted to overshadow increases in precipitation (Horton et al., 2014; Wuebbles et al., 2014; USGCRP, 2018). Increases in CDD would lower soil respiration as soils would reach their wilting point more frequently. Extreme soil moisture events will be more prevalent in the future, making soil moisture potential a more important factor of soil respiration.

Methods

Study Area

I measured growing season soil CO_2 fluxes and the microclimate (temperature and moisture) from June to October in 2018, at two locations within a first-order catchment of the

Archer Creek Watershed (135 ha), located within Huntington Wildlife Forest (HWF; 43°59'N, 74°14'W) in Newcomb, New York (USA; Figure 1). Between the years of 1981-2010, the mean temperature between June and October was 19.62°C and the mean total precipitation was approximately 508.25 mm (Table 1; accessed March 20, 2018, https://w2.weather.gov/climate/xmacis.php?wfo=btv; The National Weather Service (NWS), 2018). Subcatchment S14 (3.5 ha) has a mean elevation of 619 m, mean slope of 16°, a mean aspect of 200° (SSW) and typically has a stair-step topography with steep sided hallows. The upland forest soils are generally < 1.0 m thick and classified as Becket-Mundal series sandy loams (course-loamy, mixed, frigid, typic Haplorthods) with approximately 75% sand and less than 10% clay with many cobblestones and boulders present (Somers, 1986; Christopher et al., 2006). The soils in the S14 catchment where sampling was conducted have a high pH (5.5) compared to most Adirondack forest soils (pH < 4.5) and therefore are well buffered against acid deposition (Christopher et al., 2006; Beier et al., 2012; Homan et al., 2016). The overstory vegetation within the catchment is dominated by sugar maple (*Acer saccharum* Marsh.), white ash (*Fraxinus americana L.*), and American basswood (*Tilia americana L.*; Beier et al., 2012).

I selected two sites within S14 to establish measurement plots: a forested wetland (seep) above the first-order stream, and a mesic forest on the upper hillslope adjacent to the wetland. Located in close proximity but with differing drainage conditions, the sites were selected to compare soil microclimate and CO_2 fluxes in a mesic, well-drained soil and a relatively hydric, poorly-drained soil within the same catena. At each site, five plots were installed with gas flux sampling collars and automated sensors to continuously measure soil moisture, soil temperature and air temperature. Each plot (collar and sensor arrays) was

located a random distance between 2-4 m from a center point, where the moisture probe data logger was located. These varying distances were used to account for spatial heterogeneity within the site, and to estimate site-level mean fluxes over time and among sites (Figure 2).

Soil CO_2 Flux

Soil CO_2 flux was measured using a LI-COR LI-8100A Survey System that consists of a 20 cm dynamic flow chamber coupled with an infrared gas analyzer (IRGA; LI-COR, 2018). The specifications of the LI-8100A Survey System are provided in Appendix A. The IRGA and survey chamber were controlled by the LI-8100A application running on an Android phone via a wireless router. Three 12-volt rechargeable lead-acid batteries were used to power the IRGA for an entire day, with each battery lasting approximately 3-4 hours under typical warm summer conditions (batteries drained more quickly at temperatures < 50F). A five-minute measurement period was employed, which included a 50- second 'dead band' to allow conditions to stabilize, and followed by a 30-second line purge. Measurements began in the headwater wetland and then preceded directly to the upper hillslope, with plots being measured in the same order each time. Soil collars were made out of 20 cm diameter, schedule 40 PVC pipe, cut into 11 to 12 cm sections and beveled on the inside of one end. On June 13th 2018, prior to sampling, the beveled end of each collar was inserted a few centimeters into the soil (to achieve a firm footing while minimizing fine root damage) and the chamber offset was recorded to account for the full volume of air under the chamber once positioned on the collar.

Soil CO_2 flux measurements were made every two weeks for a total of 10 dates as follows: June 23rd, July 7th, July 21st, August 4th, August 18th, September 1st, September 15th, September 29th, October 13th, and October 27th. On each sampling day, measurements of the

complete circuit of 10 collars began at 0600 and were repeated every three hours with the final measurements starting at 1800, for a total of 5 measurements per plot per sampling day. In addition, a 24-hour diurnal sampling period was conducted to confirm that subcanopy soil temperatures are less variable diurnally, causing less diurnal variability in the flux (Fetcher et al., 1985; Chen et al., 1993; Davidson et al., 1998). The same three-hour interval was used, starting at 0600 on August 18th with the final round of measurements beginning at 0600 on August 19th 2019 (9 measurements per plot). Each plot was expected to have a total of 54 soil CO_2 flux measurements at the end of the study period.

Soil Microclimate Monitoring

Temperature sensor arrays consisted of Thermochron iButtons (model #DS1922L and #DS1921G-F5) with a range of -40°C to 85°C, resolution settings of either 0.5°C (for both models) or 0.0625°C (for #DS1922L only), and storage of 2-8 kB depending on settings and model (Maxim Integrated, 2018). The iButtons were arranged vertically on a solid PVC rod within a sealed PVC housing (6.35 cm diameter pipe) buried partially in the soil, attached to a steel reinforcement stake for stability. Within the housing, the iButtons were spaced 0.2 m apart vertically from each other, ranging from -0.2 m (below soil surface) to +1.0 m (above soil surface); note the arrays utilized did not contain sensors at the +0.8 m position. These arrays allowed for the measurement of both soil and air temperature, with the iButtons at -0.2 m and 0 m set at a 0.0625°C resolution (#DS1922L) and the others set to a 0.5°C resolution (#DS1921G-F5). Arrays were carefully installed to ensure that the 0 m iButtons were located at the surface of the soil. Sensors were programmed to record every 4 hours from June 13th at 1200 to October 30th at 0800.

Soil moisture was measured for each plot using ECH_2O GS 1 data-logging soil volumetric water content (VWC) probes connected to an ECH_2O Em50 data logger at each site (METER Group, 2018). The probes record a range of 0 to 0.57 m^3/m^3, with a resolution of 0.001 m^3/m^3, and a volume of influence of 690 cm^3. The probes were installed at -0.2 m below the soil surface at each plot and connected to the data-logger via 5-meter cables housed in 1.27 cm diameter PVC pipe conduits. Soil moisture probes were programmed to record mean conditions every 2 hours starting June 22nd at 1400 till October 30th at 1200. In each plot the buried temperature array's PVC housing and the soil moisture probe were installed at a minimum distance of 30 cm apart to avoid sampling interference.

To estimate C, N and moisture content of soils in measurement plots, samples of the O and A horizon were collected from underneath the plot collars at the end of the study period (October 30, 2018). An additional 10 randomly located soil samples were collected within each site using a 4 cm diameter soil corer to represent the soil matrix around and between the plots. These random samples were bulked together by site prior to analysis. The twelve samples (one from each of 10 measurement plots, 1 bulked sample from each site outside of plots) were analyzed for gravimetric water content, total C and total N. To calculate the gravimetric water content, 250 g wet weight samples were dried in a drying oven at 105°C for 48 hours and then weighed again. For the C:N analysis, 40 mg sub-samples were pulverized and mixed using a SPEX Mixer/Mill (8000M) to obtain fine particles. Samples were then measured by the Dumas Method of dry combustion (Thermo Scientific Flash Elemental Analyzer, 1112 series) to determine the percentage of C and N. A piece of decaying wood found buried in the soil directly beneath one collar (U3) was placed in a drying oven at 60°C for 48 hours to obtain a dry weight.

Meteorological Data

In addition to the soil microclimate measurements in the plots, first-order meteorological stations located at HWF in Newcomb were used for real-time meteorological data. A New York State (NYS) Mesonet weather station is located in a maintained clearing – which contains instruments for several other monitoring programs including National Atmospheric Deposition Program and the US Environmental Protection Agency Clean Air Status and Trends Network – approximately 4 km from the study area in Archer Creek Watershed. The Mesonet station has automated sensors that measure ambient meteorological conditions every 3-30 seconds and records / reports 5-minute means of these values. Data obtained from this station included air temperature (°C) at 2 m, soil temperature (°C) at -0.25 m, 5-minute precipitation (mm), and 24-hour precipitation (mm; NYS Mesonet, 2018). Weather instruments located in a forest opening approximately 50 m from the headwater wetland site were also used; the Ackerman Clearing tower was installed in 2007 and serves as a meteorological station for the upper Arbutus watershed, recording data every 15 minutes, including temperature (°C; Campbell Scientific model 107-I) and 15-minute precipitation (mm; Campbell Scientific model TE525WS-L; SUNY ESF, 2018). Temperature (record starting in 1986) and precipitation (record starting in 1959) data were used from the NWS station located in HWF for analysis and comparison.

Storm Events

Storm events were defined as the top 1% of daily precipitation totals based on the metrological record from the NWS station in Newcomb, NY. This threshold would allow for a few measured samples of a potentially saturated well-drained soils, to investigate how high soil

moisture impeded soil respiration and suppresses soil CO_2 flux. A statistical analysis of Newcomb's precipitation data from 1959 to 2017 found that the top 1% of daily total precipitation for the months of June through October was 37.99 mm or greater (NWS, 2018). To determine if a storm event was likely to occur, several precipitation forecasts (NYS Mesonet, North American Mesoscale Model, Global Forecast System) were monitored for 24h rainfall predictions greater than the 37.99 mm threshold. If a storm event qualified, then soil CO_2 flux would have been measured, but no such rainfall occurred at HWF during my study period.

Data Analysis

Temperature means and variance were analyzed to evaluate differences between the subcanopy microclimate (1 m above forest floor) and ambient air temperatures recorded by weather stations located in a forest gap (Ackerman Clearing) and a maintained open clearing (Mesonet station). The subcanopy temperatures analyzed were based on the mean of all five +1.0 m iButtons in the arrays installed at the two soil gas flux study sites in S14. Linear interpolation between measurement intervals was used to estimate soil temperature and moisture at a 60 sec resolution for the entire study period to allow for simultaneous comparison of observations. Tukey's multiple comparison test was used to examine if means differed among the plot level soil CO_2 fluxes. Means and variance were calculated and compared for soil temperature (-0.2 m depth), soil moisture, and the soil CO_2 flux at the site level. Two sample t-test (95% confidence) were run to test for significant differences between the sites means of soil temperature, soil moisture, soil CO_2 flux, and soil carbon and nitrogen content.

Relationships between subsurface observations of the soil microclimate (temperature and moisture at -0.2 m depth) were analyzed with correlation tests and a series of regression models. Soil moisture effects on soil CO_2 flux were initially evaluated using linear regression models based on three sets of antecedent mean soil moisture observations (24, 48 and 72 hours prior to sampling time) to account for potential lags. Pearson correlations and simple linear least-squares regressions were used to evaluate plot-level relationships between soil CO_2 flux and soil temperature. A log-linear model based on the Arrhenius equation from Lloyd & Taylor (1994) was used to examine the plot-level temperature dependence and relative reaction rates of soil respiration:

$$\ln(R) = a + b*(1/Ts) \quad [1]$$

where R is the soil CO_2 flux in µmol/m^2/s, Ts is soil temperature in degrees K, a is the intercept and b is the slope. The activation energy of the soil CO_2 flux at each plot was calculated by using the slopes from equation [1], which is equal to $-E_a/r$, where E_a is the activation energy in J/mol K and r is the gas constant (8.314 J/mol K; Lloyd & Taylor, 1994; Davidson & Janssens, 2006). The Q_{10} was calculated from the activation energy by using equation [10] from Zaragoza-Castell et al. (2008):

$$Q_{10} = e\left(\frac{10E_a}{rT^2}\right) \quad [2]$$

where E_a is the activation energy, r is the gas constant, and T is soil temperature in K. A soil temperature of 15°C was used based on the global mean soil temperature observed during the June-October 2018 study period.

A nonlinear mixed effects (NLME) regression method was used to generate a predictive model of CO_2 flux, based on repeated measures of the same ten plots located in two sites

(upland and wetland), as a function of the soil microclimate. A random effect was assigned to 'plot' that was zero-centered with normally distributed variance around the intercept using an unstructured covariance structure. This is to account for plot-level variation due to the individualized plots, calculating the residuals from the mean of the plot. Random intercepts and slopes of soil microclimate factors were incorporated to have a maximal random effect structure to achieve conditional independence. The combination of random slopes and intercepts minimize type I & II errors by avoiding a narrow confidence interval, allowing for between-individual variation in slope to be considered, accounting for all possible individual variation in the data (Schielzeth & Frostmeier, 2009; Barr et al., 2013; Winter, 2013; Harrison et al., 2018). Consequently, random intercepts and slopes can make the model too complex (overfitted) for the given data. Two nonlinear models from Davidson et al. (2012) were used to evaluate the combined effects of soil temperature and soil moisture on soil CO_2 flux. A purely Q_{10} model was fit by using equation [8] from Davidson et al. (2012):

$$R = R_{ref}(Q^{\left(\frac{Ts-10}{10}\right)}) \quad [3]$$

and a Q_{10} and water content model was fit using equation [9] from Davidson et al. (2012):

$$R = R_{ref}(D^{\left(M_{opt}-M\right)^2})(Q^{\left(\frac{Ts-10}{10}\right)}) \quad [4]$$

where R is the soil CO_2 flux in µmol/m^2/s, Ts is soil temperature in °C, R_{ref} is the reference R at 10 °C, Q is the Q_{10} parameter, M is soil moisture in %, M_{opt} is the optimum soil moisture which is set at the maximum % soil moisture content encountered in the data, and D is a calibrated parameter. Equation [4] was used for both instantaneous soil moisture and 72-hour antecedent soil moisture. The nonlinear models were compared using Akaike Information Criterion (AIC). AIC compares models from given data by considering the model's goodness of fit (based on a

likelihood function) and a plenty for adding more parameters (overfitting). The model with the lower AIC would be the preferred model for the given data set, unlike R^2, which explains how much of the variance of the dependent variable is explained by variables in a regression model (Akaike, 1978). Random R_{ref} coefficients were regressed with soil %C and %N to identify potential effects of C and N content on CO_2 flux rates. The NLME models were fitted to the data using the nlmer function from the lme4 package in R 3.6.1 (Bates, 2007; R Development Core Team, 2019).

A linear mixed effects (LME) regression method was used to generate a predictive model of CO_2 flux, to account for potential heteroscedasticity in the nonlinear models. Using equation [1], all combinations of the explanatory variables of site and soil elemental content (carbon and nitrogen) were used to best fit the data to a model based on AIC. The LME model was fitted to the data using the lmer function from the lme4 package in R 3.6.1 (Bates, 2007; R Development Core Team, 2019). The log-linear relationship causes issues fitting other variables to the model other than soil CO_2 flux and temperature. To account for this, the intercept from the plot level log-linear temperature-CO_2 flux models were regressed with soil %C and %N to identify potential effects of C and N content on CO_2 flux rates. I also evaluated potential relationships of antecedent soil moisture with the residuals of the plot level log-linear regression fits, to determine if model error was associated with moisture extremes. For example, a temperature model may overestimate flux when soils are very dry and respiration becomes moisture-limited. Likewise, fully saturated soils where gas exchange becomes impeded, may have an overestimated flux. The nonlinear and log-linear models were compared by using a Jacobian transformation on the log-linear model's AIC (Akaike, 1978).

I used the log-linear LME model (equation [1]) to forecast potential changes in flux resulting from projections of future temperature change, based on downscaled global circulation model ensembles (CMIP5; Pierce et al. 2014). The model was run with adjusted temperature data reflecting generalized changes in temperature from the recent past. The baseline dataset was constructed of the mean daily temperature during the nominal growing season (June 1st through October 31st) based on weather records from NWS Newcomb, NY station from 1981-2010. These temperature 'normals' were then adjusted by the forecasted changes (Δt) derived from the CMIP5 downscaled predictions for Essex County, New York (USA), for two future endpoints (2050 and 2090) and under RCP 4.5 (low emissions) and RCP 8.5 (high emissions) scenarios relative to the 1971-2000 temperature 'normals'. Because the Δt values from CMIP5 predictions were seasonally estimated (accessed 10 April 2019 at www.nyclimatescience.org; The New York Climate Change Mapping Tool, 2019), the summer Δt were applied to June, July and August baseline data, while the fall Δt were applied to September and October baseline data (Table 2). With the derived Δt downscaled to match weather stations in open fields and the log-linear model based on subcanopy soil temperatures, the forecasted weather station temperatures were converted to forecasted subcanopy air temperatures based on the empirical relationship observed at HWF between the air temperatures measured at the Mesonet station and the temperature sensors at the study sites. The forecasted subcanopy air temperatures were then converted to forecasted soil temperatures based on the empirical relationship observed at HWF between air and soil temperature sensors at the study sites.

Using the log-linear model, an uncertainty analysis was conducted to investigate the uncertainty of the model parameters in predicting the future soil CO_2 flux. Bootstrapping was used to sample from a multivariate normal distribution of the model parameters (slope and intercept) using their standard errors and the covariance matrix from the model (Raftery et al., 1993; Vrugt et al., 2003; Wilby, 2005). Since the temperature sensitivity of soil respiration has been shown to not significantly change with warmer temperatures (Carey et al., 2016), a Monte Carlo analysis (10,000 iterations) was used to predict the changes in the future soil CO_2 flux compared to the NWS Newcomb thirty-year average temperatures. This was done under the assumption that all other factors (e.g., labile carbon pool size, rate of photosynthesis, forest composition and structure, etc.) remain unchanged and that there are no soil moisture limitations. All analyses described above and graphics were performed using R 3.6.1 (R Development Core Team, 2019).

Results

Soil CO_2 Flux

The mean soil CO_2 flux was roughly equivalent in the headwater wetland (3.38 µmol/m^2/s) and upper hillslope sites (3.61 µmol/m^2/s) in Archer Creek watershed (two-sided t-test, p = 0.116). I did observe significant differences in mean flux rates between plots (Table 3), with overall more significant variation among the upper hillslope plots, while only one of the wetland plots differed significantly from the other wetland plots (Figure 3). The highest flux measured was 10.02 µmol/m^2/s at plot U3 on September 15th at 1558, and the lowest was 0.43 µmol/m^2/s at plot U2 on October 27th at 0959. Fluxes at all plots increase from June 23rd until August 4th, after which they started to decline, with the exception of a noticeable decrease in

the upper hillslope plots on July 21st and a notable increase on September 15th (Figure 4). Soil CO_2 flux fluctuated more so on a weekly timescale than a diurnal timescale, as soil temperatures remain steady and vary over longer timeframes. The diurnal measurement confirmed there was no significant changes in the soil CO_2 fluxes over the daily interval. From August 18th at 0600 to August 19th at 0600, the fluxes had a mean CV of 7.41%, while soil temperatures had a mean CV of 1.89%, falling by approximately 1°C during the 24-hour study (Figure 5).

Soil Microclimate

Soil temperatures were not significantly different among the sites (t-test, $p = 0.723$). Mean soil temperatures were 14.03°C in the headwater wetland and 14.08°C in the upper hillslope (Table 4). Site soil temperatures were averaged from all five -0.2 m iButtons per site. Soil temperature and soil CO_2 flux were positively correlated ($r = 0.57$, $p < 0.001$), with the observed temperature dependence of the soil CO_2 flux having an exponential relationship (Figure 6).

Soil moisture (VWC) was significantly greater but less variable in the wetland site relative to the upland site (t-test, $p = 0.003$). The headwater wetland had a mean VWC of 0.416 m^3/m^3, while the upper hillslope had a mean VWC of 0.229 m^3/m^3 (Table 5). Soil moisture varied more in the upper hillslope (CV = 29.694%) than it did in the headwater wetland (CV = 17.548%). The sites were wettest on average in October, and were at their driest in late August, early September (Figure 7; Figure 8). The headwater wetland plots had a mean gravimetric water content of 2.18 g/g, with the upper hillslope plots having a mean of 0.59 g/g (Table 6). Soil moisture was negatively correlated with soil CO_2 flux ($r = -0.06$, $p = 0.162$), and with soil

temperature (r = -0.12, p = 0.006). The 72-hour antecedent soil moisture had the best correlation (Pearson's r) with the soil CO_2 flux (Table 7).

Soil carbon and nitrogen were significantly greater in the headwater wetland site (t-test, p = 0.002, p < 0.001 respectively; Figure 9). Plot H1 had significantly lower C and N than the other four wetland plots, while Plot U2 had the lowest C and N content seen across both sites (Table 6). A 108.5g (dry weight) piece of decaying wood, which had white rot fungus on it, was found directly underneath one of the upland collars (U3).

Meteorological Data

The mean monthly temperatures and monthly precipitation from the weather stations (Ackerman, Mesonet, and NWS) and the temperature arrays were compared with the thirty-year average from NWS Newcomb, NY (Table 8). The mean air temperatures for the headwater wetland and upper hillslope were lower than the weather stations and experienced smaller variance. Based on the NWS data, the month of July was 1.56 °C warmer than average, August was 2.28 °C warmer than average and September was 2.17 °C warmer than average. In contrast June was 1.33 °C colder than average and October was 1.50°C colder than average. The month of June had 29.72 mm below average rainfall, July had 27.69 mm below average rainfall and the month of August had 51.02 mm below average rainfall (greater than 1 standard deviation). The month of September experience 11.94 mm above average rainfall and October was close to average rainfall (+2.54 mm). There was a moderate drought from early July until early November, with a severe drought from the beginning of September until the middle of October (accessed March 27, 2019, https://www.ncdc.noaa.gov/temp-and-precip/drought/weekly-palmers/20180901; The National Oceanic and Atmospheric Administration (NOAA), 2019;

accessed March 20, 2019, https://droughtmonitor.unl.edu/Maps/MapArchive.aspx; The National Drought Mitigation Center, University of Nebraska-Lincoln (NDMC), 2019a, 2019b).

Soil CO_2 Flux Modeling

The plot level temperature dependence, activation energy and Q_{10} of soil CO_2 flux (derived from the log-linear models) varied between plots, with each having a high adjusted R^2 (Table 9). The NLME regression using the Q_{10} function produced the following population model from the fixed effects:

$$R = 1.861(3.852^{\left(\frac{Ts-10}{10}\right)}) \quad [5]$$

with an AIC = 1006.45 and a Pseudo-R^2 for the fixed effect = 0.54 (n = 525; Figure 10). The NLME regression using the Q_{10} and instantaneous soil moisture function produced the following population model from the fixed effects:

$$R = 1.887(1.000^{\left(M_{opt}-M\right)^2})(3.881^{\left(\frac{Ts-10}{10}\right)}) \quad [6]$$

with an AIC = 1007.69 and a Pseudo-R^2 for the fixed effect = 0.63 (n = 525). The NLME regression using the Q_{10} and 72-hour antecedent soil moisture function produced the following population model from the fixed effects:

$$R = 1.929(0.999^{\left(M_{opt}-M\right)^2})(4.095^{\left(\frac{Ts-10}{10}\right)}) \quad [7]$$

with an AIC = 1001.17 and a Pseudo-R^2 for the fixed effect = 0.66 (n = 525; Figure 11). The population models were based on the random effect of 'plot' and the random coefficients of R_{ref} and Q_{10} (Table 10). Residuals from all three models show signs of heteroscedasticity and are further discussed in the discussion section. Based on AIC, there was no difference between the Q_{10} model and the Q_{10} and instantaneous moisture models. The Q_{10} and 72-hour antecedent

soil moisture model had the lowest AIC, making it the preferred model. Soil C and N were not considered in these models but were compared to the random R_{ref} coefficients of the Q_{10} model and the Q_{10} and 72-hour antecedent soil moisture model. Weak negative linear relationships were exhibited for carbon content (Q_{10} adjusted R^2 = -0.04, Q_{10} and 72-hour antecedent adjusted R^2 = -0.09) and nitrogen content (Q_{10} adjusted R^2 = -0.07, Q_{10} and 72-hour antecedent adjusted R^2 = -0.10)).

The fitted LME models were compared using AIC, with the difference in AIC being less than three (Table 11). Such small differences are not significant and would not support choosing a more complex model over a simpler one (Burnham & Anderson 2004; Davidson et al., 2012). The preferred model based on AIC had soil temperature as the only explanatory variable, giving the following population model from the fixed effects:

$$\ln(R) = 39.381 - 10998.214*(1/Ts) \quad [8]$$

with an AIC = -360.51, mean square error (MSE) = 0.025, root mean square error (RMSE) = 0.157 and a Pseudo-R^2 for the fixed effect = 0.48 (n = 525; Figure 12). The population model was based on the random effect of 'plot' and the random coefficients of soil temperature, which were similarly to the plot level log-linear models (Table 12). The activation energy of soil CO_2 flux at S14 was equal to 91.45 KJ/ mol K (95% CI [83.97, 99.02 KJ/ mol K]). The Q_{10} was found to be 3.76 (95% CI [3.37, 4.20]).

Soil carbon and nitrogen were not significant in the model based on AIC, but were compared to the plot level log-linear model intercepts due to the use of a log-linear transformation equation. Strong positive linear relationships were exhibited for carbon content (intercepts adjusted R^2 = 0.71; Figure 13) and nitrogen content (intercepts adjusted R^2 = 0.69).

Soil moisture was not considered in the linear model due to the log-linear transformation, but the 72-hour antecedent soil moisture was compared to the plot level log-linear model residuals to determine if model error was associated with moisture extremes. There was no distinct pattern that showed a clear effect of soil moisture that could explain the residuals in the log-linear models.

A Jacobian transformation was used on the log-linear LME model's AIC to be able to compare to the nonlinear models. The transformed AIC (806.32) was the lowest AIC of all four models, making the log-linear LME model the preferred model for this study.

Future Soil CO_2 Flux Uncertainty Analysis

The forecasted weather station temperatures and the NWS thirty-year average temperatures were converted to forecasted subcanopy air temperatures using the following equation based on the empirical relationship observed at HWF between the air temperatures measured at the Mesonet station and the temperature sensors at the study sites:

$$STa = 0.943 + 0.907(MTa) \quad [9]$$

where STa is the sites air temperature in °C, MTa is the Mesonet air temperature in °C, and the adjusted $R^2 = 0.95$. The forecasted subcanopy air temperatures were covert to forecasted soil temperatures using the following equation based on the empirical relationship observed at HWF between the soil and air temperature sensors at the study sites:

$$Ts = 8.913 + 0.346(Ta) \quad [10]$$

where Ts is site soil temperature in °C, Ta is site air temperature in °C, and the adjusted $R^2 = 0.64$. The log-linear LME model was used to then predict soil CO_2 fluxes from the forecasted soil temperatures. The uncertainty analysis of the mean soil CO_2 flux from June 1st to October 31st

for the thirty-year average and future emission scenarios, predicts soil CO_2 flux to increase by 0.29 µmoles/m^2/s by 2090 under scenario RCP 4.5 and by 0.70 µmoles/m^2/s by 2090 under scenario RCP 8.5 (Table 13; Figure 14).

Measurement Errors and Corrections

Due to colder weather on the last sampling day of October 27th, battery failure prevented the completion of the final round of measurements at 1800. This led to each plot having a total of 53 soil CO_2 flux measurements. After the temperature array data were collected, it was noted that the recording interval for the -0.2 m iButton in array N was consistently 44 minutes off from the remaining iButtons during the study period.

Wildlife interfered with soil moisture probe cables several times leading to gaps in the data. Wildlife were able to unplug all probes in the headwater wetland on September 7th around 2000 and probes were plugged back in on September 15th just after 0600. Wildlife were able to unplug all probes in the headwater wetland again on September 28th around 2000 and probes were plugged back in on September 29th just before 0600. Wildlife also chewed through a cable for plot U3 soil moisture probe (port 5) in the upper hillslope on September 15th around 1600, the cable was repaired and plugged back in on September 17Th at 1400. Data are missing for all probes affected between these time frames. Due to this each model considered a sample size of 525, as all five headwater wetland plots were missing antecedent soil moisture at 0600 on September 15.

From data analysis, it was noted that the response of some of the probes were adversely affected from being unplugged, registering unusually high readings. Headwater wetland Plot H1 (Port 1) was reading above 0.65 m^3/m^3, when it usually read between the 0.40

m^3/m^3 to 0.20 m^3/m^3, after being plugged back in on September 17th until it was unplugged again on September 28th. Headwater wetland Plot H4 (Port 3) was reading above 0.65 m^3/m^3 as well, where it usually read between 0.50 m^3/m^3 to 0.40 m^3/m^3, and seemed to be having issues with the data logger registering it was plugged in, after it was plugged back in on September 29th till October 27th. A bias correction was done on the affected data based on the means of Plots H2, H3 and H5 for Plot H3, as they were generally close throughout the season, and means of all plots were used for Plot H1, as it was generally always below the other ports.

A couple of readings were incorrect due to being chewed through or plugged back in, registering extremely low or negative values. The readings shortly after these low values were normal and other ports did not have any significant changes in their readings between those two-time frames. A bias correction was used to fix these readings by replacing the off reading with the reading just after it, if it was after being plugged back in, or just before it, if it was because of being chewed on. The readings affected were the headwater wetlands' Plot H1 (Port 1) on September 18th at 0800 and 1000, Plot H2 (Port 5) on September 18th at 0800, Plot H3 (Port 4) on September 29th at 0800, and the upper hillslopes' Plot U3 (Port 5) and Plot U4 (Port 1) on September 15th at 1600.

Discussion

Soil temperature was the best predictor variable for the soil CO_2 flux based on the data collected. There were significant differences between soil moisture and soil carbon between the sites, but there were no significant differences in the soil CO_2 flux. There were significant differences in soil CO_2 flux between the plots. Soil moisture had an effect on soil CO_2 flux based on the Q_{10} and 72-hour antecedent nonlinear model, but it was very close to one. Conditions

did not get wet enough during measurements to impact the soil CO_2 flux and the driest condition were missed by measurements. The moderate to strong collinearity between temperature and soil moisture made it difficult to separate any effects of soil moisture on the soil CO_2 flux. Carbon did appear to influence the intercept of the plot level models, but was not significant in the log-linear LME model. The log-linear LME soil model was the preferred models based on AIC.

Soil CO_2 Flux Modeling

The NLME models were used to examine the effects of soil moisture on soil CO_2 flux. Using the Q_{10} function as a comparison, the Q_{10} and instantaneous soil moisture function did not improve the model as the AIC for the two models were similar. The calibrated parameter for soil moisture (D) was close to 1 (0.9999) suggesting that there was a minor effect of soil moisture on soil CO_2 flux during the study. The Q_{10} and 72-hour antecedent soil moisture function has the lowest AIC of the NLME models, though the calibrated parameter D is still close to 1 (0.9998). The Q_{10} and 72-hour antecedent soil moisture function indicates a minimal effect of soil moisture on soil CO_2, while the comparison of the residuals from the plot level log-linear models showed no clear effect of soil moisture.

All of the NLME models exhibit signs of heteroscedasticity, with greater variance in the residuals under warmer conditions (Figure 15). This increase in variance can be attributed to the argument that the Q_{10} function itself is temperature dependent, with higher values found in colder climates/conditions, and that the relationship between respiration and temperature is not simply exponential as other factors can influence this relationship (Lloyd & Taylor, 1994; Davidson et al., 1998; Schipper et al., 2014). Temperate regions experience seasonal variation,

where summers are often warm and dry, and winters are cold and wet (Savage & Davidson, 2001). Calibrating a model to a full year worth of data in this case can cause systemic seasonal errors, though the use of seasonally variable parameters can help improve the model (Davidson et al., 2012). A simple option to correct for heteroscedasticity would be a log transformation and the log-linear model residuals have constant variance (Figure 16). The log transformation made it difficult to add other variables to the model, though the soil elemental content appeared to influence the intercepts. To be able to compare a nonlinear and a transformed model, a Jacobian transformation needs to be applied to the log-linear model's AIC (Akaike, 1978). The resulting AIC was lowest of all the models, making the log-linear model the preferred model for this study.

Soil Temperature and Q_{10}

The present study confirmed that soil temperature and soil CO_2 flux have a strong positive relationship. The plot level log-linear models using only soil temperature had high adjusted R^2 (0.79 - 0.95; Table 9) and could effectively explain soil CO_2 flux. Soil temperature was relatively similar among all plots but there were significantly differences between some of the plots' soil CO_2 fluxes. The four headwater wetland plots (H2-H5) had very similar fluxes throughout the study (Tukey's grouping c). These four headwater wetland plots had four of the five highest activation energy and Q_{10}, with Plot H4 had the highest activation energy and Q_{10} (Table 9). Plot U3 had a similar activation energy and Q_{10} value to the lowest plot (H3) in the headwater wetland grouping, and was the highest of the upper hillslope. Plots U4 and U5 (Tukey's grouping e) had similar fluxes, and had the next highest activation energy and Q_{10} values. Plots H1 and U2 (Tukey's grouping f) had the lowest fluxes, activation energy and Q_{10}

values (Table 9). In the Normal QQ plot of the log-linear model random intercepts, Plot H4 fell above the normal residual line, and Plots H1 and U2 fell below the line (Figure 17).

Some studies have been previously conducted at Archer Creek Watershed on the relationship of the soil CO_2 flux with temperature and other factors (Richey, 1994; McHale et al., 1998; Gross, 2012; Gomez, 2014). These studies had confirmed the strong positive relationship of the soil CO_2 flux with temperature. Richey (1994) had positive Pearson correlation for soil temperature and the soil flux with a Pearson's r = 0.694 in 1992 and a Pearson's r = 0.418 in 1993. Gomez (2014) found a significant positive correlation of soil temperature with the soil flux, having a Spearman ρ for his study sites ranging from 0.49 to 0.83. McHale et al. (1998) had strong positive Pearson correlation as well for soil temperature and the soil flux with a Pearson's r = 0.68 in 1993 and Pearson's r = 0.69 in 1994. My study had similar Pearson's r to Richey (1994) and McHale et al. (1998), where Pearson's r for the headwater wetland, upper hillslope and S14 were 0.70, 0.49 and 0.57 respectively. The disparities observed with some of these studies are likely explained by the different protocols (e.g., static versus dynamic chamber) and sampling designs (e.g., intensive, single-season versus extensive year-round). This study was only conducted in the growing season similar to the other studies (Richey, 1994; McHale et al. 1998; Gross, 2012), but continued measurements should be made year-round to better capture the variations in the flux like Gomez (2014). This study also had more temporal measurements and fine scale spatial measurements compared to the other studies, that had more spatial coverage and less temporal.

Comparing Q_{10} values across sites can be difficult due to a range of factors, including soil moisture, nutrient content, organic material, microbial and root respiration, and depth at which

soil temperature was measured (Davidson et al., 2006; Davidson & Janssens, 2006). The mean Q_{10} estimated for this study was 3.76 (95% CI [3.37, 4.20]), with plot level Q_{10} ranging from 2.91 to 5.37. This study was not significantly different to the Q_{10} reported by Davidson et al. (1998) at Harvard Forest, but was significantly higher than those reported by Fahey et al. (2005) for Bear Brook and Watershed 1 experimental sites in Hubbard Brook Experimental Forest (Figure 18). Median global Q_{10} has been reported as 2.40, with a reported range from different biomes of 1.10 to 3.30 (Raich & Schlesinger, 1992). The mean Q_{10} in the Northeast was calculated to be approximately 3.33 (based on mean Q_{10} reported from: my study; Davidson et al., 1998; McHale et al., 1998; Fahey et al., 2005; Davidson et al., 2006; Giasson et al., 2013) and falls at the highest end of the global range. Measurements of Q_{10} in the forest ecosystems of the Northeast are thought to be higher than the global mean due to the increase in temperatures seen during the growing season, and increased root growth and respiration during the spring and summer months (Raich & Schlesinger, 1992; Davidson et al., 1998). Differences in Q_{10} among these sites can be explained by site specific conditions, different methodologies and the temperature dependence of the Q_{10} function (Lloyd & Taylor, 1994; Davidson et al., 1998; Davidson et al., 2006; Davidson & Janssens, 2006; Schipper et al., 2014). Davidson et al. (2006) estimated a spring and fall Q_{10} for Howland Forest in Maine of 3.50 and 2.50 respectively, displaying this issue at a single site. Spring would have a higher Q_{10} than fall due to the springtime root growth, and soil temperatures warm from the top down (temperature is measured at a fixed depth), while CO_2 is produced at varying depths. Several studies, including my own, have only sampled during one growing season. For an accurate Q_{10}, a year-round, multi-year study would be needed to accurately capture as many conditions as possible and the

use of seasonally variable parameters should be considered. Further research should be conducted to account for all these potential variations to better understand the Q_{10} of Archer Creek Watershed soils.

Carbon Content

Soil carbon content was a potential explanatory factor for soil CO_2 flux due to its relationship with the intercepts of the plot level log-linear models (Figure 13). The lowest soil CO_2 fluxes came from the two plots with the lowest soil C (plots H1 and U2). The four headwater wetland plots (H2 - H5) had the highest carbon content, with Plot H4 having the highest at 32.68% (Table 6). However, the highest soil CO_2 flux did not come from Plot H4 or the headwater wetland plots. Plots U1 and U3 had the largest mean soil CO_2 fluxes, but had significantly lower soil C than the four headwater wetland plots, 8.71% and 8.63% respectively. Plot U1 had the third lowest intercept and activation energy among all plots, while Plot U3 had an intercept and activation energy more closely related to the headwater wetland groupings (Table 9). Plot U3's high flux and similarities to the four headwater wetland plots can be explained by the decaying piece of wood underneath the collar providing extra organic material. Plot U3 had two dates where the CO_2 fluxes were significantly higher than expected, and fell above the 2 standardized residuals based on RMSE of the log-linear LME model (Figure 16). However, the reason for Plot U1's high flux but low activation energy is not known. There could potentially be organic material that was not found providing extra carbon to the plot or another factor that was influencing soil CO_2 flux. Further analysis would need to conducted in that plot to determine why the soil CO_2 flux was as high as observed. Furthermore, Plot U5's soil CO_2 flux was found to not be significantly different from Plots H3 and H5, while it had the

third lowest carbon content (7.26%). These mixed results (Figure 19), along with relatively low replication, may explain why soil C was not significant in the model. Although soil C appeared to influence the intercept of the temperature-flux relationship and activation energy of the underlying reactions, it was not found to be a consistent predictor of the flux after accounting for temperature.

Soil Moisture and Microclimatic Conditions

Soil moisture was not identified as a predictor variable of soil CO_2 flux based on my data. The Q_{10} and 72-hour antecedent soil moisture function indicated a minor effect of soil moisture as the calibrated parameter D was close to 1 (0.9998). In comparison with all models, the log-linear LME model was the preferred model based on AIC. The 72-hour antecedent soil moisture comparison with the residuals of the log-linear model showed no clear effect of soil moisture. Since soil CO_2 flux measurements during extremes in soil moisture were not well captured during the study, it was hard to parse apart the effects of soil moisture from soil temperatures because of its negative collinearity with soil temperature (Table 7). Also, temperature was a suitable predictor (high plot level adjusted R^2) of explaining soil CO_2 flux. What the soil moisture data are showing is more of a relation to the soil temperature than with the soil flux.

Soil moisture did fluctuate throughout the months of July to September especially in the upper hillslope. There was some significant drying down in all of the upper hillslope plots, with four of five plots dropping below 0.200 m^3/m^3 on five measurement dates; two of those plots approached 0.100 m^3/m^3 on four of those dates (Figure 8). Two plots in the headwater wetlands also decrease by approximately 0.200 m^3/m^3 over this time period (Figure 7). Soil moisture anomalies of 20 to 40 mm below average occurred in the month of July (below 30th

percentile), and anomalies of 40 to 60 mm below average occurred in August through October (below 20th percentile), based on the Land Surface Monitoring and Prediction CPC 'Leaky Bucket Model' relative to the 1951 to present time period. The model estimates soil moisture, evaporation, runoff, and potential evaporation from observed temperature and precipitation (accessed April 1, 2019, https://www.cpc.ncep.noaa.gov/products/Soilmst_Monitoring/index.shtml; NWS, 2019). Surface soil moisture and root zone soil moisture were below the 20th percentile, relative to the 1948 to 2009 time period, reaching at times as low as below 2nd percentile during July and September. Groundwater was below the 30th percentile, relative to the 1948 to 2009 time period, reaching at times below the 5th percentile during September. These data were obtained from NASA's Gravity Recovery and Climate Experiment (GRACE) satellites, which detect small changes in the Earth's gravity field caused by the redistribution of water on and beneath the land surface. The data are modeled from measurements from GRACE along with meteorological data (precipitation, temperature, solar radiation) to create a long-term record of soil moisture and groundwater (accessed 26 March 2019, https://nasagrace.unl.edu/Archive.aspx; NASA, 2019).

The summer of 2018 was substantially warmer than normal in the US Northeast, with the mean temperatures in July and September being above the 95th percentile and above the 99th percentile in August, based on station observed monthly mean surface air temperatures at a 0.5 x 0.5 degree resolution since 1948 (NWS, 2019). August 2018 was the warmest August recorded by the NWS station in Newcomb, NY (1986 - present). The 2018 growing season was also relatively dry, with below-average precipitation from May to August. August 2018 had the 5th lowest total rainfall recorded in August at the NWS station in Newcomb, NY (1959 - present).

Well above normal temperatures along with abnormally dry conditions led to moderate drought conditions existing from July through October, with severe drought conditions existing throughout the month of September (NDMC, 2019b). During September, stream gauges dropped below the lower 25th percentile in the region (NDMC, 2019a). Lastly, during the month of September, the Palmer Drought Severity Index (PDSI) indicated that moderate drought conditions existed in HWF (NOAA, 2019). Overall, these relatively dry and warm conditions could explain why the headwater wetland had marginally higher fluxes than the upland, because fluxes in the upper hillslope may have been lower due to respiration being moisture limitation. During drier conditions, well-drained soils can approach the wilting point while poorly drained soils are likely experience more favorable conditions for gas exchange (Davidson et al., 1998; Ullah & Moore, 2011).

Ambient drought conditions were evident in the 2-hour soil moisture measurements, especially in well-drained soils of the upper hillslope site (Figure 8). Unfortunately, the study was set up to track extreme rain events and not significant dry downs, so the soil CO_2 flux was not measured during these significantly dry periods. The set schedule of measurements missed most of these dry days but did capture the end of the first major dry-down period. Measurements were made on July 21st which was a hot and dry day, with no significant rainfall since July 6th, and storms were expected overnight. Upon further inspection, there is a clear decrease in the flux in all plots in the upper hillslope and a slight decrease in a few of the headwater wetland plots. Most of the flux measurements made on July 21st in the upper hillslope were approximately two standard deviations below the seasonal mean flux (Figure 16). In the normal QQ plot, these points fell below the normal line, with the measurements falling in

the -3 to -2 Theoretical Quantiles range, as the model overestimated flux by an average of 45.37% for the upper hillslope on July 21st. Although this suggested that soil moisture could have been a limiting, July 21st was not the lowest soil moisture recorded during flux measurements.

Soil flux measurements made on September 1st coincided with lower observed soil moisture than July 21st, but the upper hillslope fluxes did not appear to be moisture-limited, based on the overall better model estimates (1.12% error on September 1st vs. 45.37% error on July 21st). The September 1st sampling coincided with the lowest soil moisture observed at measurement time for all but two plots, but two days prior to the sampling date it rained approximately 10 mm, which briefly rewetted the soil at -0.20 m depth (Figure 7; Figure 8). The September 1st sampling may indicate the effect of rewetting on dry soils known as the Birch effect, when precipitation results in a pulse of respiration and corresponding soil CO_2 flux after a prolonged dry period (Birch, 1958; Lee et al., 2002; Yuste et al., 2003; Xu et al., 2004; C. W. Harper et al., 2005; Warren, 2014, 2016). Soil moisture may have been a limiting factor of the CO_2 flux, but this threshold was not adequately captured during this study. Although ambient weather conditions were categorized as drought, I found only limited evidence to indicate that conditions became dry enough to limit soil respiration (and therefore CO_2 flux).

Soil CO_2 Flux Predictions

The Mesonet network has good geographic coverage across the Adirondacks (18 stations). All of the Mesonet stations in the Adirondacks record soil temperature, which is not typical of weather stations. If one wanted to use the log-linear LME model to estimate the soil CO_2 flux for sites similar to my headwater wetland and upper hillslope around the Adirondacks,

then the Mesonet measured soil temperatures could be used to predict the sites soil temperatures. The soil temperatures measured by the Mesonet (-0.25 m) at HWF and the soil temperatures measured at my sites had a strong positive correlation (Pearson r = 0.97). Soil temperatures for similar sites in the Adirondacks could be predicted by using the closest Mesonet stations' measured soil temperatures with the following equation, based on the empirical relationship observed at HWF between the Mesonet station and the temperature sensors at the study sites:

$$STs = -4.042 + 1.054(MTs) \quad [11]$$

where STs is the sites soil temperature in °C, MTs is the Mesonet soil temperature in °C, and the adjusted $R^2 = 0.95$. Soil temperatures below the forest canopy were on average 4.04°C cooler than in the open field where Mesonet was located. Equation [11] could be used to predict the soil temperature at sites in the Adirondacks by using the closest Mesonet station, to provide estimates of in-situ temperature for soil CO_2 flux prediction at similar forest sites.

For use of the model outside of areas that have available soil temperature data, the model could still be used, if measured air temperature at weather stations could be empirically related to the soil temperature under the canopy. As expected, the daily maximum temperatures in the subcanopy at the sites were lesser, and the daily minimum temperatures were greater, than those recorded by Mesonet station located in open field (Fetcher et al., 1985; Chen et al., 1993; Strong et al., 1997; K. A. Harper et al., 2005), and most weather stations do not measure soil temperature in contrast to the Mesonet stations. Future analysis should be conducted to predict soil temperatures in a forested site from air temperatures in an open field. A major factor that would need to be considered is the effect of solar radiation on

air temperature in an open field. If a correction for that can be used to accurately predict air temperature under the canopy and then the log-linear LME model could be used in other similar locations. This would be immensely useful and something that future research should focus on to help better understand and estimate the soil CO_2 flux from available data.

Using the estimated ΔT to forecast subcanopy soil temperatures and the assumption that all other factors will remain unchanged, the future soil CO_2 flux was predicted using the log-linear LME model. Under the RCP 4.5 scenario, soil CO_2 flux from the study sites could increase by 10.18% over the next century. Whereas under the RCP 8.5 scenario, the soil CO_2 flux is predicted to increase by 24.28% by 2090 (Figure 20). Under both scenarios, temperatures are expected to stay warmer longer into the fall, leading to a higher predicted increase in the flux by 2090 in the fall months. It was noticed that soil CO_2 flux is expected to have a greater increase in the fall months and increase at a faster rate through the months of September and October. The expected increases could be explained by warmer temperatures being favorable for microbial activity and fine root production (McHale et al., 1998; Ryan & Law, 2005; Davidson et al., 2006; Allison & Treseder, 2008). Increases in soil CO_2 flux rates could lead to a significant increase in atmospheric CO_2 and depletion of organic carbon matter from soils in the future (Raich & Schlesinger, 1992; Schlesinger & Andrews, 2000).

Increasing temperatures are expected to increase soil CO_2 flux, but many other factors will influence how much it increases. Soil moisture is the primary factor that could affect soil respiration as moisture limitations could occur more often under warming conditions. Model forecasts are predicting longer dry periods between rain events (CDD) and a potential increase in short term droughts in the US Northeast (Sillmann et al. 2013; Singh et al. 2013; Horton et al.,

2014; Wuebbles et al., 2014; USGCRP, 2018). Warmer temperatures are expected to increase evapotranspiration, and could alter the timing of snow melt and the start of the growing season. If increases in precipitation are not enough to offset these changes, soils could dry out more often during the warmer months, producing short term droughts. Moisture limitations are known to constrain respiration (Davidson et al., 1998; Knapp et al., 2002; Yuste et al., 2003; Xu et al., 2004; C. W. Harper et al., 2005), so an increase in prolonged dry periods, like the summer of 2018, could decrease the future flux. When all factors are considered (moisture limitations, shifts in physiological response, depletion of liable C pools, etc.), there could be a neutral or negative response to warming (Carey et al., 2016). All factors that can directly impact soil CO_2 flux need to be included in a model to accurately forecast changes in the future flux.

Future Research into Changes to the Soil CO_2 flux due to Climate Change

Adjustments to the current methodology may be warranted. For example, my data suggest that three daily measurements, made twice a month, at 0800, 1200 and 1600, would have sufficiently sampled the flux under varying daily temperatures. Reducing the frequency of sampling at a given site would allow for a more spatially-extensive design that could sample more of the edaphic and microclimatic variability in the study watershed.

Along with sampling at regular intervals, future work to examine in-situ soil moisture thresholds for respiration and CO_2 flux can be made more effective by monitoring the 'real-time' observations by autonomous sensors and sampling during key periods, or 'events', when soils are either very dry or fully saturated. In most locations this would be possible by deploying data loggers with cellular network connectivity, however, at the HWF study site located in the remote Adirondacks, network coverage is very poor. In this specific case, we could explore the

use of the existing tower and radio infrastructure (at Ackerman Clearing) that transmits real-time data to an online database where it can be accessed remotely. Although unique to the HWF Archer Creek watershed site, it may be sufficient to monitor the stage and discharge data from the stream weirs, which is recorded and visualized online in 15-min intervals, to identify event sampling periods. Similarly, soil moisture data from weather stations like Mesonet could be monitored to identify and effectively sample moisture extremes at remote field sites.

Conclusion

The soil microclimate exerts control over soil CO_2 flux primarily through soil temperature, with potential influence from soil moisture and carbon content. Soil temperature was the main predictor of the soil CO_2 flux during the study. The soil moisture threshold was not captured during the study, as the correlation between soil moisture and soil temperature made it hard to tease apart the effects of soil moisture. The relationship between the soil CO_2 flux, temperature and moisture was studied with a dynamic chamber and intensive, in-situ measurements, to better understand their interactions. Soil CO_2 flux had a strong positive relationship with soil temperature and a Q_{10} value of 3.76 was found through modeling of the temperature-flux interaction. Soil moisture did have a moderate negative relationship with the soil CO_2 flux but this was possibly due to the correlation between soil moisture and soil temperature. The Q_{10} and soil moisture functions indicated a minor effect of soil moisture, but model comparison led to the log-linear LME model being the preferred model. Comparisons of soil moisture to the residuals of the log-linear models did not show a clear effect of soil moisture on the flux. The soil CO_2 flux, soil moisture and carbon content varied across plots under nearly identical soil temperature conditions, indicating that spatial heterogeneity in

other factors may influence soil CO_2 flux. Finding the soil moisture threshold, along with the impacts that soil organic material, microbial and ecosystem composition, land use history, and other factors have on the soil respiration are needed to better understand and predict soil CO_2 flux.

The study period encompassed a cool start to a significantly hot and dry summer, which turned into a cold and wet fall. Soil moisture was low through much of the months of August and September, due to significantly high temperatures and below average rainfall over the months of May to August. Drought conditions existed most of the summer with severe drought conditions occurring in September. While the fixed sampling interval did not produce measurements during the driest periods observed via soil moisture sensors, soil CO_2 flux did not seem to be negatively influenced by low soil moisture. With the Adirondacks having mesic conditions, soil moisture may not be a limiting factor on the flux, except for potentially in the extreme ranges (Davidson et al., 1998; Knapp et al., 2002; Yuste et al., 2003; Xu et al., 2004; Harper C. W. et al., 2005). Low soil moisture and the amount of days removed from last rain event could be factors affecting the flux, as the driest day was predicted well by the log-linear LME model. With warmer temperatures, heavier rain events and short-term drought predicted in the future (Griffiths & Bradley, 2007; DeGaetano, 2009; Brown et al., 2010; Horton et al., 2014; USGCRP, 2018), the flux needs to be more intensely studied under these conditions to better understand what other factors affect the relationship between the soil CO_2 flux and temperature.

Table 1 - June to October monthly climatological data (mean precipitation (mm), mean minimum temperature (°C), mean maximum temperature (°C) and mean temperatures (°C)) for Newcomb, New York. Based on the NOAA 1981-2010 thirty-year climate normals.

Month	Mean Precipitation	Mean Maximum Temperature	Mean Minimum Temperature	Mean Temperature
June	98.55	21.72	9.94	15.83
July	102.87	23.89	12.17	18.06
August	99.57	22.56	11.61	17.11
September	99.82	18.22	7.67	12.94
October	107.44	11.72	1.33	6.50

Table 2 - Forecasted changes (Δt) derived from the CMIP5 downscaled predictions for Essex County, New York (USA) in Summer (June, July, August) and Fall (September, October, November) by 2050 and 2090 under RCP 8.5 (high emissions) and RCP 4.5 (low emissions) scenarios relative to the 1971-2000 temperature 'normals'.

Season	Emissions Scenario	Change in Temperature (°C) by 2050	Change in Temperature (°C) by 2090
Summer	RCP 8.5	2.2	5.1
	RCP 4.5	1.8	2.8
Fall	RCP 8.5	2.4	5.2
	RCP 4.5	2.1	3.0

Table 3 - Daily means, plot mean and standard deviations of the soil CO_2 flux (µmoles/m^2/s) for each plot. Tukey's multiple comparison groupings is listed for each plot, plots with different letters had significantly different means.

Date	H1	H2	H3	H4	H5	U1	U2	U3	U4	U5
6/23/18	1.71	3.13	2.99	2.80	2.78	4.42	1.53	4.09	2.09	2.33
7/7/18	1.61	3.97	3.74	3.96	3.27	5.44	1.68	5.30	2.74	2.77
7/21/18	1.75	3.76	3.47	4.21	3.40	3.62	1.30	4.32	1.97	2.08
8/4/18	2.47	5.87	5.57	6.67	5.23	6.83	2.53	7.93	4.27	4.00
8/18/18	2.32	5.09	4.59	5.22	4.48	6.63	2.17	7.31	3.67	3.95
9/1/18	2.00	4.57	3.91	5.03	4.26	5.56	2.06	7.04	2.85	3.68
9/15/18	1.92	5.31	4.19	4.88	4.13	5.97	2.38	9.43	3.23	3.77
9/29/18	1.14	3.23	2.45	2.80	2.57	3.95	1.46	6.00	1.83	2.31
10/13/18	1.04	2.58	2.53	2.55	2.21	3.15	1.22	3.91	1.50	1.78
10/27/18	0.63	1.08	1.02	0.99	0.95	1.71	0.60	1.54	0.82	0.89
Mean	1.73	4.00	3.58	4.07	3.46	4.93	1.75	5.89	2.62	2.88
Standard Deviation	0.57	1.33	1.19	1.54	1.17	1.58	0.56	2.15	1.01	1.02
Tukey's Comparison	f	c	cd	c	cd	b	f	a	e	de

Table 4 - Mean monthly soil temperature (°C) and mean site soil temperature (°C) for the headwater wetland and upper hillslope. Site soil temperatures were averaged from all five -0.2 m iButtons from the temperature arrays at each site.

	Headwater Wetland	Upper Hillslope
Month	Mean Soil Temperature	Mean Soil Temperature
June	12.26	12.54
July	15.70	15.89
August	16.59	16.70
September	14.87	14.91
October	9.79	9.49
Mean June-Oct	14.03	14.08

Table 5 - Plot level mean volumetric water content (VWC; m^3/m^3), standard deviation (m^3/m^3) and coefficient of variance (%). Data missing from all plots in the headwater wetland from September 7th at 2000 to September 15th at 0800 and from September 28th at 2000 till September 29th 0600 due to wildlife interference. Data missing for Plot U3 in the upper hillslope from September 15th at 1600 to September 17th at 1400 due to wildlife interference.

	Headwater Wetland					Upper Hillslope				
Month	H1	H2	H3	H4	H5	U1	U2	U3	U4	U5
Mean	0.280	0.438	0.414	0.460	0.441	0.191	0.327	0.243	0.187	0.168
Standard Deviation	0.025	0.054	0.073	0.018	0.030	0.033	0.046	0.057	0.048	0.034
Coefficient of Variance	8.929%	12.329%	17.633%	3.913%	6.803%	17.277%	14.067%	23.457%	25.668%	20.238%

Table 6 - Plot level percent soil carbon content, percent soil nitrogen content, C:N ratio, and gravimetric water content (g/g). Soil samples taken from directly below the collars of the O and A horizons. HRAND and URAND are based on 10 randomly located core samples from the sites, bulked together as a single reference sample for the plot area.

Plot	%C	%N	C:N	Gravimetric Water Content (g/g)
H1	5.32	0.44	12.09	0.78
H2	22.77	1.85	12.31	2.50
H3	24.46	1.84	13.29	2.25
H4	32.68	2.47	13.23	2.89
H5	24.45	1.96	12.47	2.46
HRAND	9.69	0.71	13.65	0.73
U1	8.71	0.54	16.13	0.56
U2	3.92	0.27	14.52	0.47
U3	8.63	0.59	14.63	0.65
U4	9.28	0.69	13.45	0.69
U5	7.26	0.47	15.45	0.58
URAND	7.51	0.54	13.91	0.57

Table 7 - Plot level Pearson's Correlation Coefficient of soil CO_2 flux with soil moisture, soil CO_2 flux with 72-hour antecedent soil moisture, and 72-hour antecedent soil moisture with soil temperature.

Plot	Soil CO_2 Flux x Soil Moisture	Soil CO_2 Flux x 72-hour Antecedent Soil Moisture	72-hour Antecedent Soil Moisture x Soil Temperature
H1	-0.53	-0.72	-0.74
H2	-0.30	-0.54	-0.51
H3	-0.37	-0.54	-0.57
H4	-0.23	-0.57	-0.55
H5	-0.44	-0.62	-0.63
U1	-0.39	-0.58	-0.64
U2	-0.30	-0.56	-0.68
U3	-0.60	-0.67	-0.71
U4	-0.40	-0.59	-0.60
U5	-0.35	-0.63	-0.71

Table 8 - Monthly mean temperature (°C), mean study period temperature (°C), total monthly precipitation (mm), and total study period precipitation (mm) from the NWS weather station in Newcomb, NY, the Mesonet weather station at HWF, Ackerman Clearing weather station, and study sites (temperature only). Data is compared to the mean temperature (°C) and mean total precipitation (mm) from the NWS thirty-year averages for Newcomb, NY. Headwater wetland and upper hillslope temperatures averaged from all five +1.0 m iButtons from the temperature arrays at each site. Standard deviation and coefficient of variation provided for the mean temperatures.

	NWS Thirty-Year Average (1981-2010)		NWS		Mesonet		Ackerman Clearing		Headwater Wetland	Upper Hillslope
Month	Mean Temperature	Total Precipitation	Mean Temperature	Total Precipitation	Mean Temperature	Total Precipitation	Mean Temperature	Total Precipitation	Mean Temperature	Mean Temperature
June	15.83	98.55	14.50	68.83	15.10	67.14	15.29	74.93	15.60	15.73
July	18.06	102.87	19.61	75.18	19.87	74.21	20.01	73.15	19.5	19.56
August	17.11	99.57	19.39	48.51	19.20	56	19.17	52.07	18.64	18.61
September	12.94	99.82	15.11	111.76	15.10	112.62	15.03	111.76	14.60	14.62
October	6.50	107.44	5.00	109.98	6.27	111.9	5.74	131.83	5.74	5.79
Mean/ Total	14.12	508.25	14.82	409.26	15.16	421.87	15.05	443.74	14.84	14.87
Standard Deviation	4.39		6.62		7.52		7.42		7.09	6.97
Coefficient of Variance	31.09%		44.67%		49.60%		49.30%		47.78%	46.87%

Table 9 - Model coefficients (slope and intercept), adjusted R^2, activation energy with 95% CI (kJ/mol K) and Q_{10} with 95% CI for the plot level log-linear regression of soil CO_2 flux and soil temperature.

Plot	Intercept	Slope	Adj R^2	Activation Energy (kJ/mol k) (95% CI)	Q_{10} (95% CI)
H1	34.540	-9788.901	0.83	81.38 (71.19, 91.58)	3.25 (2.80, 3.77)
H2	41.888	-11653.675	0.93	96.89 (89.32, 104.45)	4.07 (3.65, 4.54)
H3	39.683	-11059.172	0.92	91.95 (84.62, 99.26)	3.79 (3.41, 4.21)
H4	49.873	-13953.625	0.93	116.01 (107.28, 124.74)	5.37 (4.73, 6.09)
H5	43.453	-12149.813	0.95	101.01 (94.34, 107.69)	4.32 (3.92, 4.76)
U1	35.631	-9792.818	0.84	81.42 (71.52, 91.31)	3.25 (2.82, 3.75)
U2	31.373	-8879.821	0.79	73.83 (63.17, 84.48)	2.91 (2.50, 3.40)
U3	40.549	-11167.554	0.79	92.85 (79.59, 106.11)	3.84 (3.17, 4.65)
U4	38.987	-10947.668	0.85	91.02 (80.25, 101.78)	3.74 (3.20, 4.37)
U5	38.464	-10769.470	0.85	89.54 (79.11, 99.97)	3.66 (3.15, 4.26)

Table 10 - Random effect coefficients for the nonlinear mixed effects models.

	Nonlinear Mixed Effects Models					
	Q_{10}		Q_{10} x Soil Moisture		Q_{10} x 72-hour Antecedent Soil Moisture	
	R_{ref}	Q_{10}	R_{ref}	Q_{10}	R_{ref}	Q_{10}
H1	0.913	3.816	0.926	3.852	0.941	4.095
H2	2.157	3.852	2.154	3.874	2.109	4.095
H3	1.880	3.859	1.880	3.884	1.857	4.095
H4	2.113	4.189	2.123	4.161	2.147	4.095
H5	1.832	3.958	1.833	3.965	1.814	4.095
U1	2.701	3.726	2.786	3.780	2.948	4.095
U2	0.893	3.726	0.896	3.778	0.883	4.095
U3	3.203	3.605	3.256	3.685	3.305	4.095
U4	1.386	3.961	1.439	3.979	1.569	4.095
U5	1.528	3.861	1.588	3.888	1.715	4.095

Table 11 - Model comparison of fitted log-linear mixed effects model ((ln)Flux ~) using Akaike Information Criterion (AIC). Models fit with lmer function from lme4 package in R 3.6.1, random effect of 'plot' with random intercept and slope of temperature (1 + (1/Temp) | Plot) used in all models.

Linear Mixed Effect Model	AIC	ΔAIC
~ (1/Temp) + (1 + (1/Temp) | Plot)	-360.51	0
~ (1/Temp) + Site + (1 + (1/Temp) | Plot)	-360.13	0.38
~ (1/Temp) + Site + C + (1 + (1/Temp) | Plot)	-359.34	1.17
~ (1/Temp) + N + C + (1 + (1/Temp) | Plot)	-359.06	1.45
~ (1/Temp) + Site + N + (1 + (1/Temp) | Plot)	-359.06	1.45
~ (1/Temp) + N + (1 + (1/Temp) | Plot)	-358.62	1.89
~ (1/Temp) + C + (1 + (1/Temp) | Plot)	-358.52	1.99
~ (1/Temp) + Site + C + N + (1 + (1/Temp) | Plot)	-357.83	2.68

Table 12 - Soil temperature random effect coefficients (intercept and slope) of the log-linear mixed effects model.

Plot	Intercept	Slope
H1	34.666	-9824.362
H2	41.625	-11578.386
H3	39.765	-11082.953
H4	47.172	-13177.623
H5	42.411	-11850.347
U1	37.461	-10318.863
U2	32.200	-9117.269
U3	41.310	-11387.122
U4	38.716	-10869.689
U5	34.666	-9824.362

Table 13 - The mean predicted soil CO_2 flux (µmoles/m^2/s) from a Monte Carlo analysis (10,000 iterations) with bootstrapping the model coefficients (intercept and slope) to account for the model uncertainty, for June 1st and October 31st.

	Predicted mean Soil CO_2 Flux (µmoles/m^2/s)				
	NWS Thirty-Year Average	RCP 4.5 Scenario		RCP 8.5 Scenario	
		2050	2090	2050	2090
Mean	2.89	3.13	3.18	3.26	3.59
Standard Deviation	0.35	0.39	0.40	0.41	0.45
Coefficient of Variation	12.23%	12.38%	12.41%	12.46%	12.66%

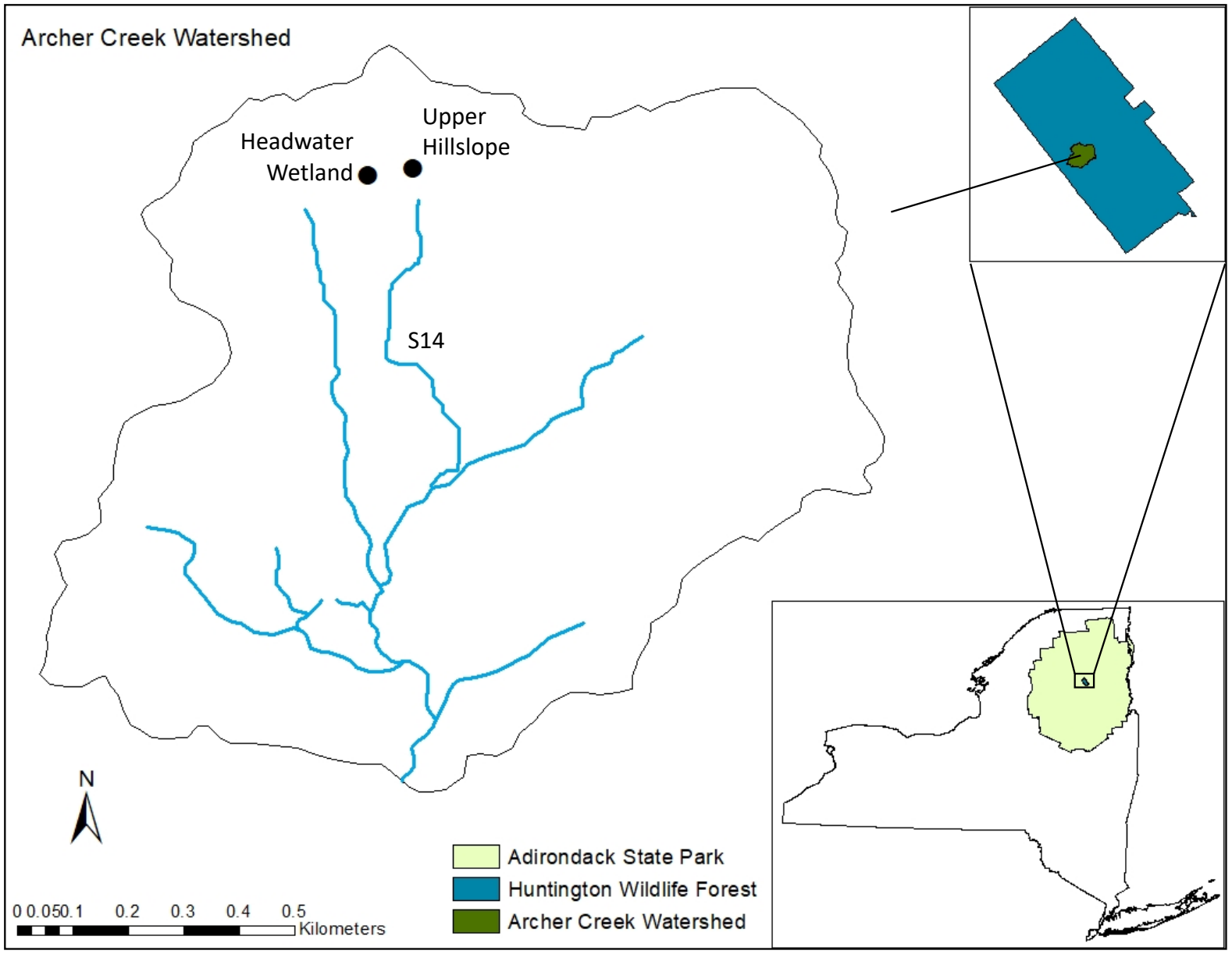

Figure 1 - The location of Archer Creek Watershed, and Subcatchment S14 headwater wetland and upper hillslope, within Huntington Wildlife Forest, in the Adirondack State Park, New York, US.

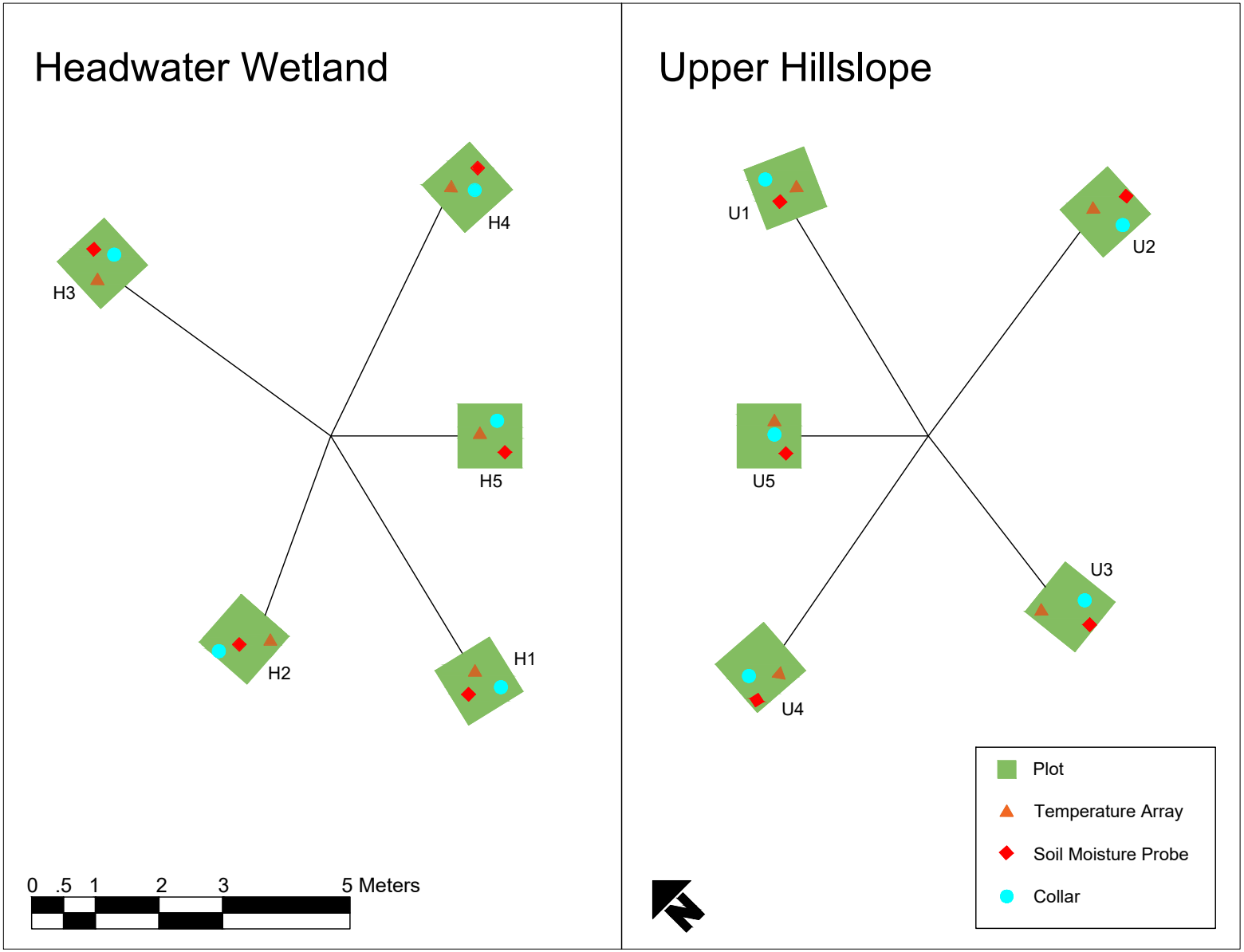

Figure 2 - Maps of site design with location of the plots (1-5), soil moisture probes, temperature arrays and soil collars. Modified from Gross (2012).

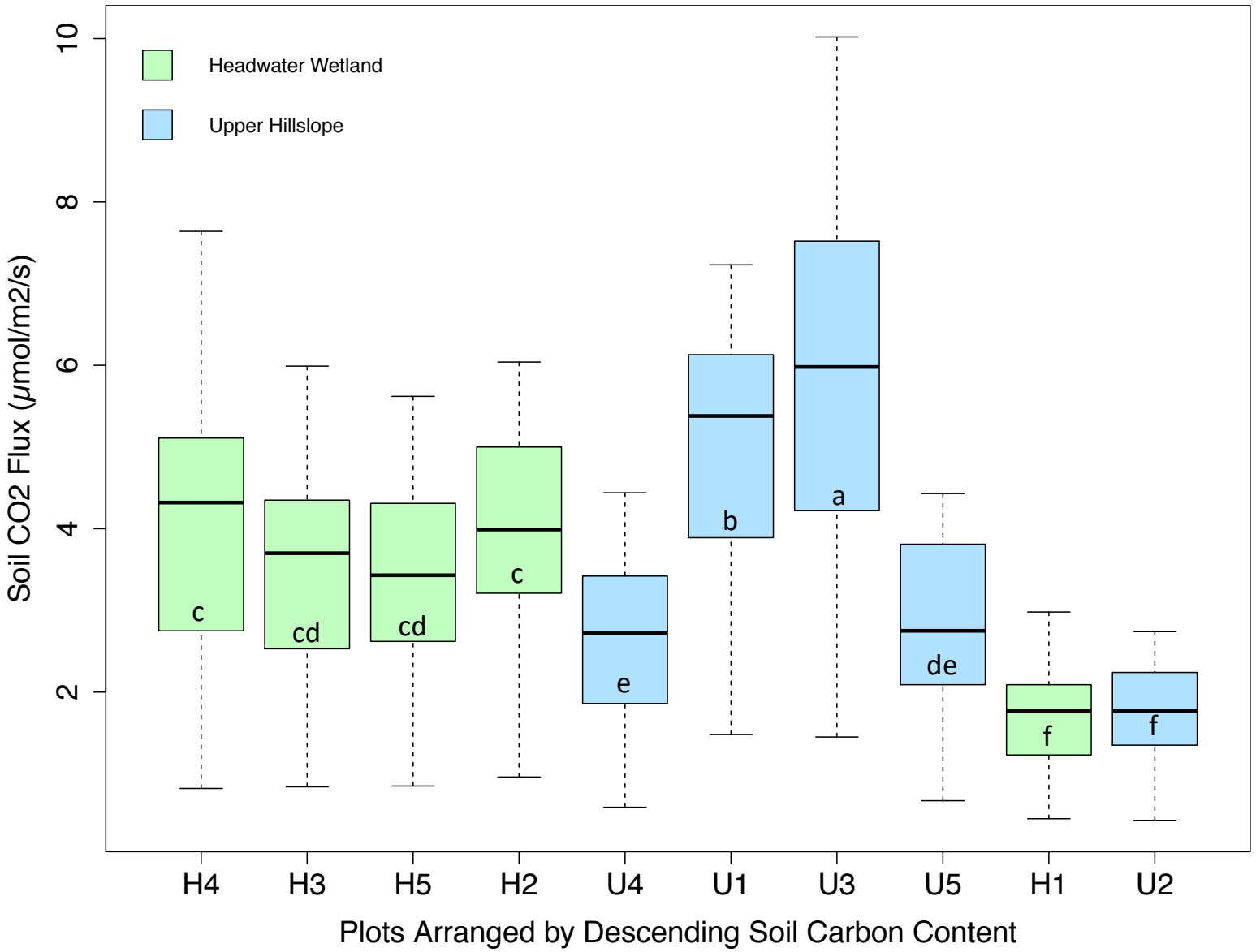

Figure 3 - Boxplots of soil CO_2 flux (µmoles/m^2/s) per plot and site during the study period, showing the distribution of the fluxes (minimum, first quartile (Q1), median, third quartile (Q3), and maximum), arranged by descending soil carbon content. Letters represents Tukey's Grouping, plots with different letters have significantly different means (n = 53 per plot).

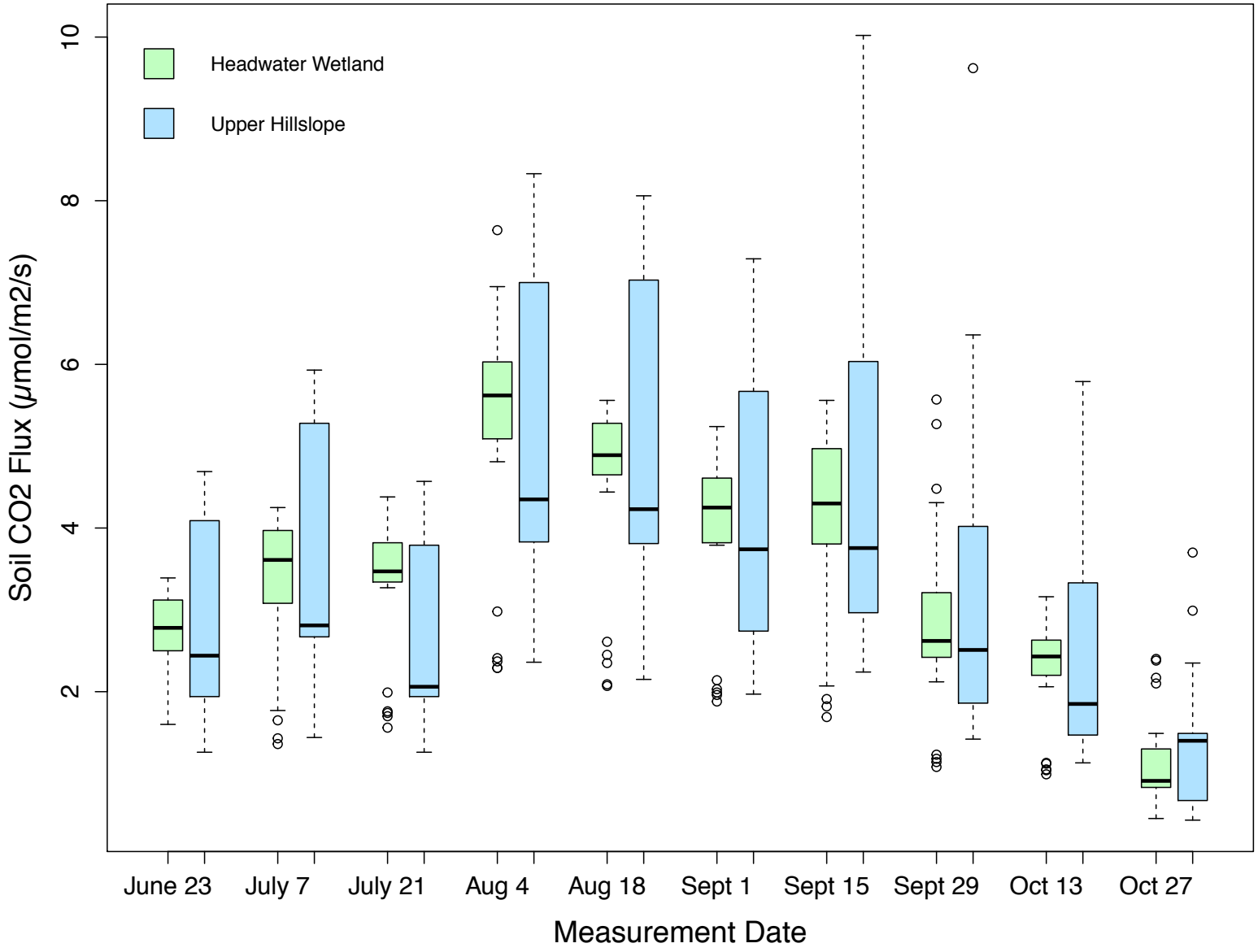

Figure 4 - Boxplots of site soil CO_2 flux (µmoles/m^2/s) by date, showing the distribution of fluxes (minimum, first quartile (Q1), median, third quartile (Q3), and maximum) over time during the study period. All dates have n= 25 per sites (August 18th 21:00 readings excluded), except October 27th, where all plots missing 18:00 measurement (n= 24 per site).

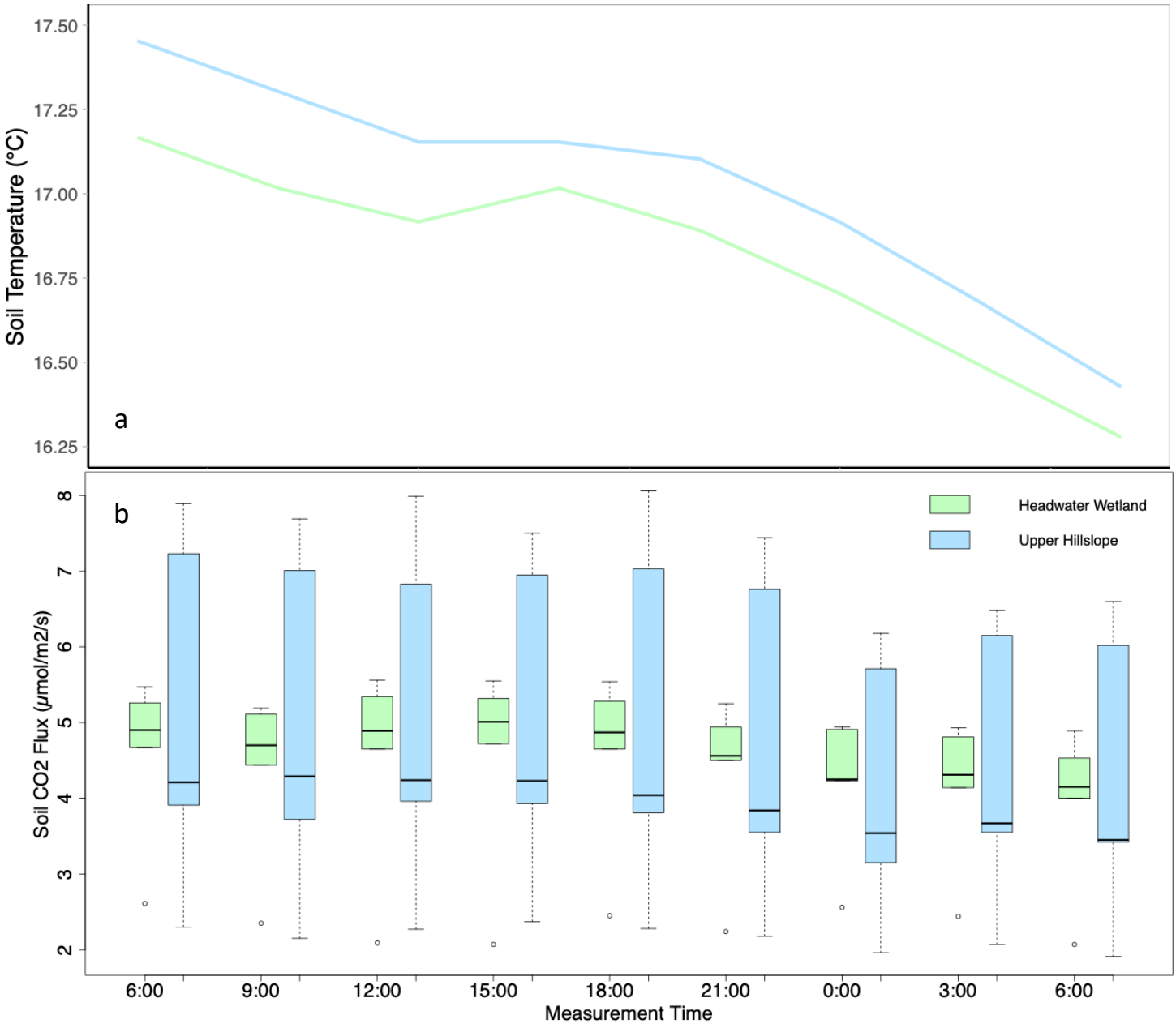

Figure 5 - Time series showing a) site mean soil temperatures (°C) and b) boxplots of the sites soil CO_2 flux (µmoles/m^2/s) at each time measurement during the diurnal study. Soil CO_2 flux measurements were made every three hours starting on August 18th at 0600 and ending on August 19th at 0600.

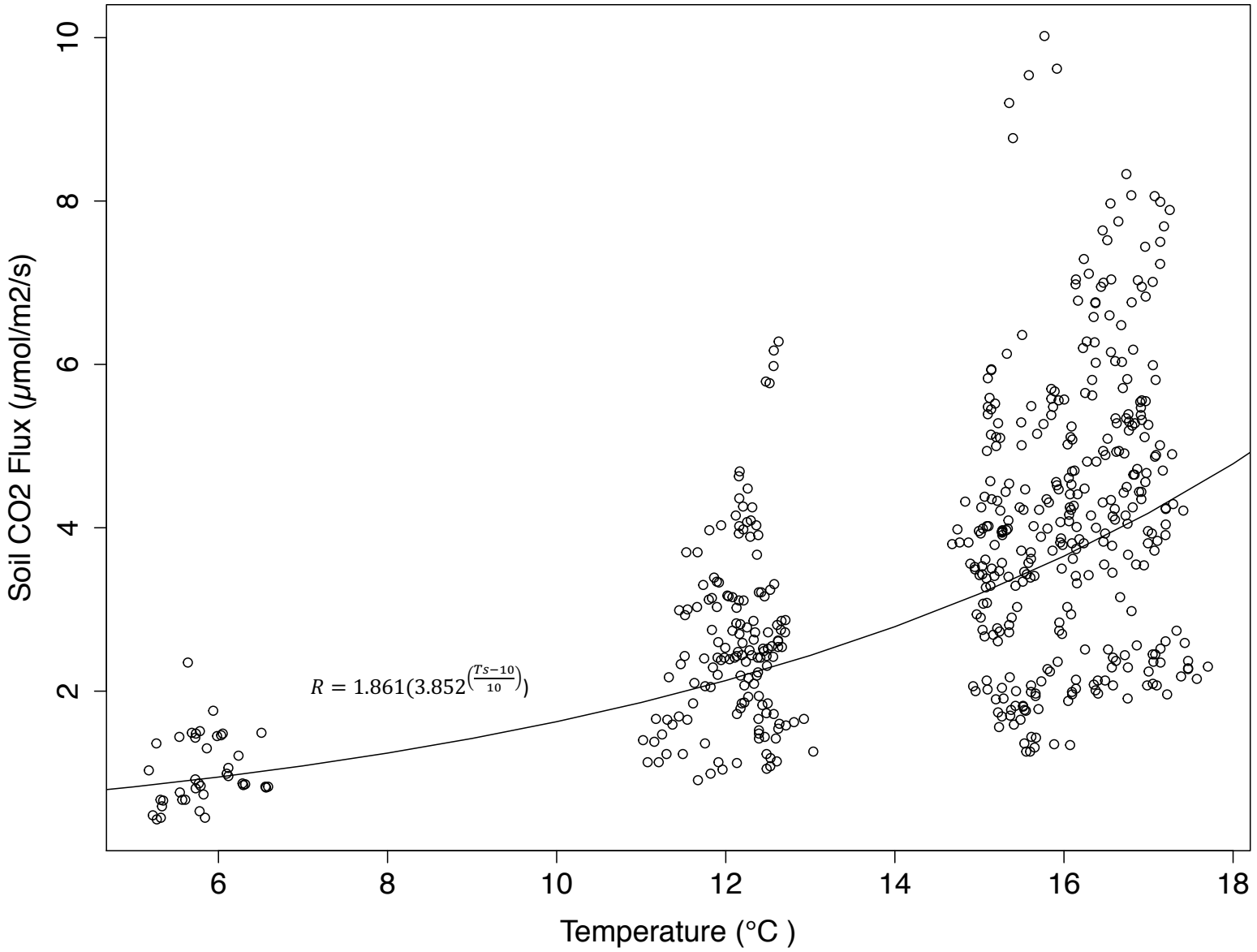

Figure 6 - Observed temperature (°C) dependence of the soil CO_2 flux (µmoles/m^2/s) in Subcatchment 14. Line fit using Q_{10} function (Pseudo R^2 = 0.54).

Figure 7 - Times series of volumetric water content (m^3/m^3) for each plot in the headwater wetland during the study period. Data missing from all plots in the headwater wetland from September 7th at 2000 to September 15th at 0800 and from September 28th at 2000 till September 29th 0600 due to wildlife interference.

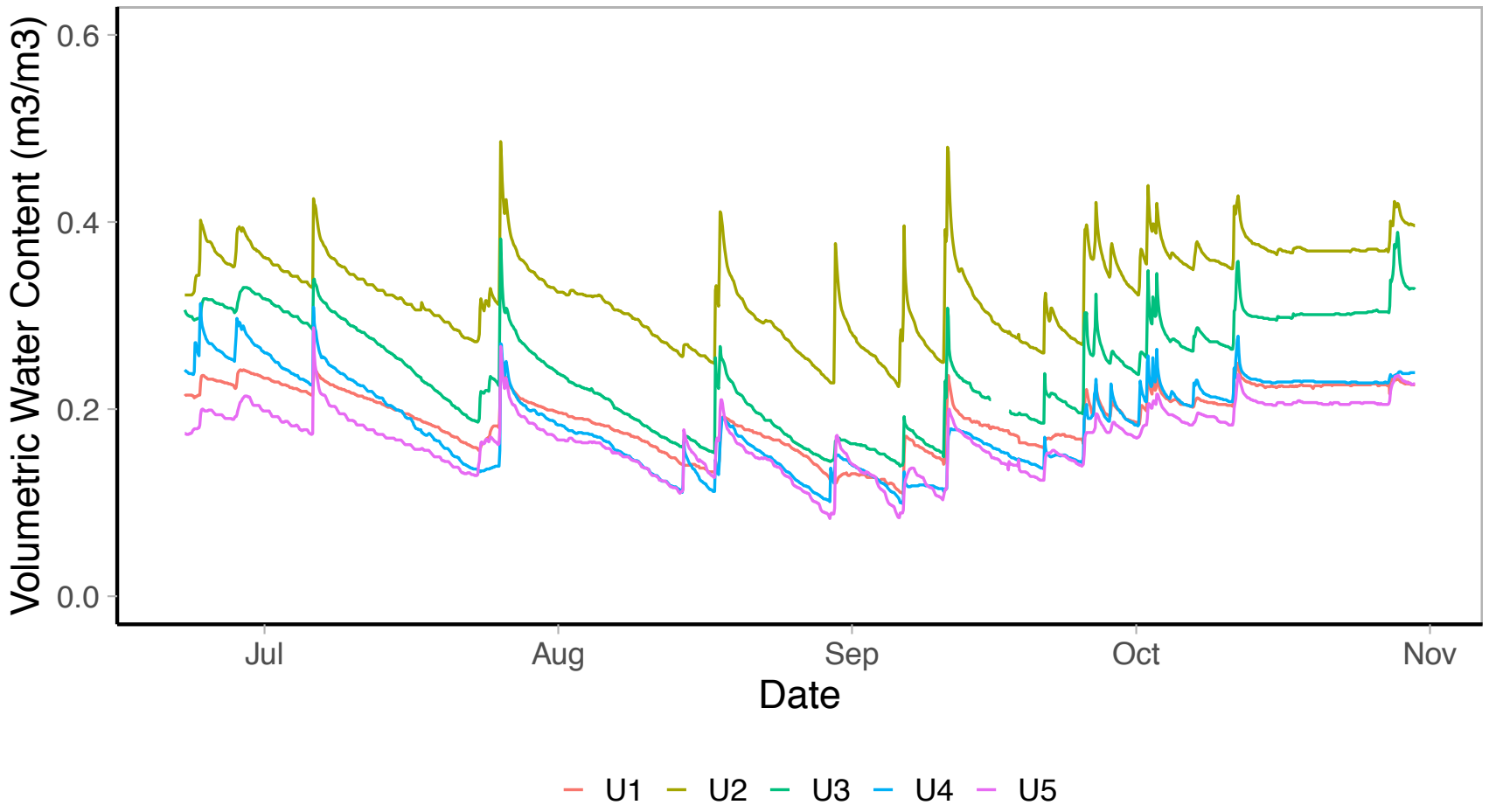

Figure 8 - Times series of volumetric water content (m^3/m^3) for each plot in the upper hillslope during the study period. Data missing for Plot U3 in the upper hillslope from September 15th at 1600 to September 17th at 1400 due to wildlife interference.

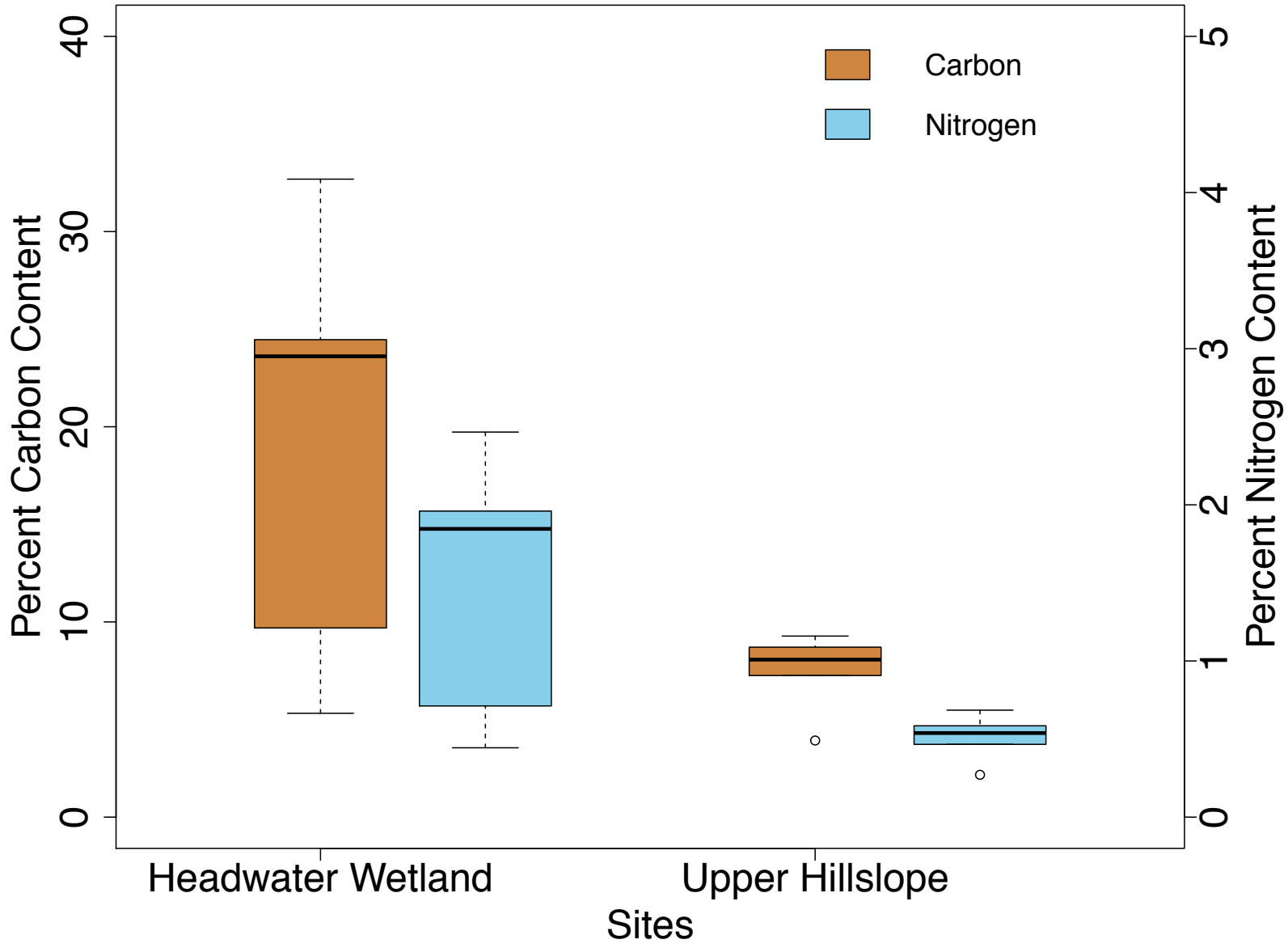

Figure 9 - Boxplots of percentage of soil carbon content and nitrogen content by site (n = 6 per soil element per site). Soil samples taken from directly below the collars of the O and A horizons. HRAND and URAND are the 10 random samples from the sites, bulked together for a reference to compare the collar soil samples to.

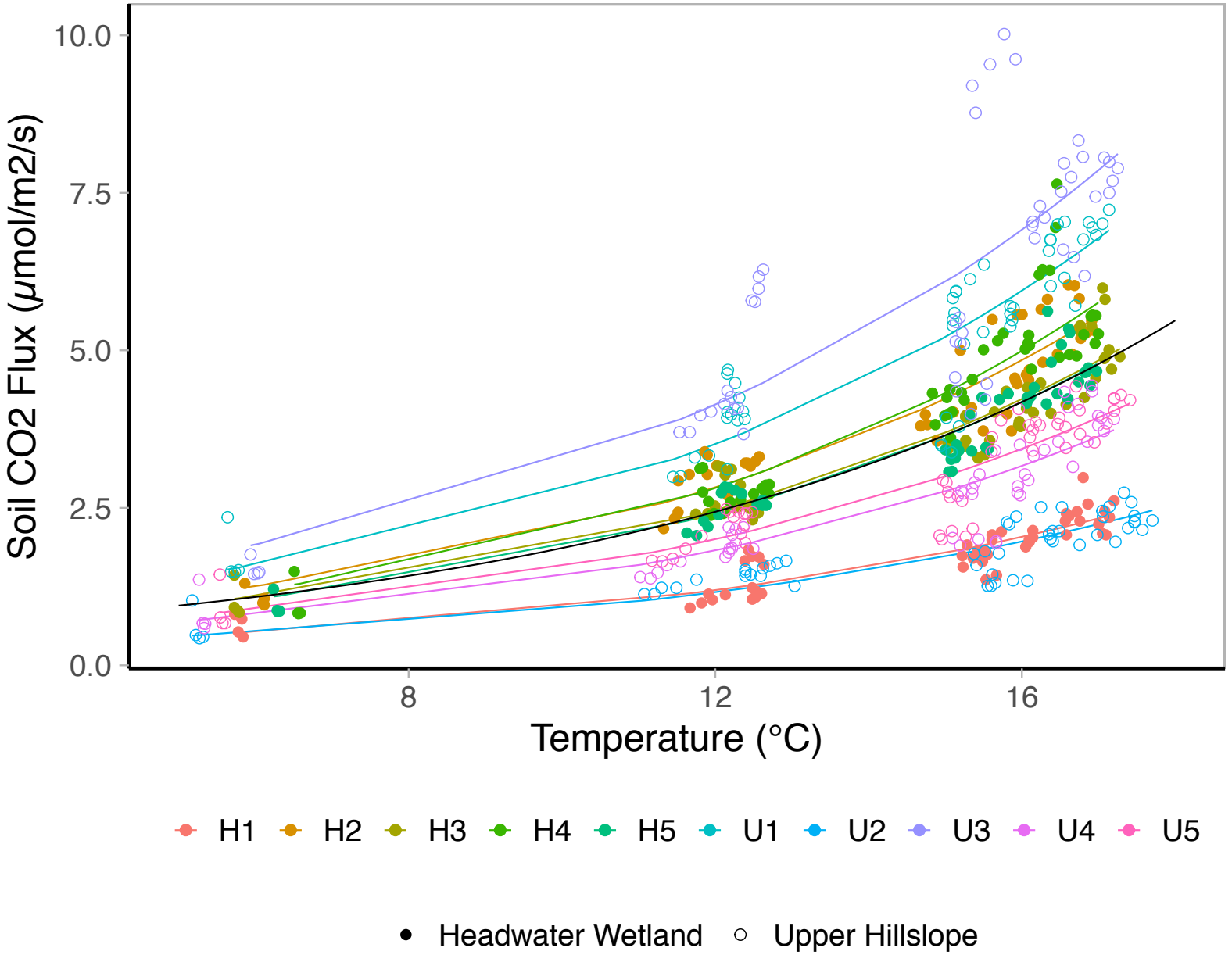

Figure 10 - Temperature dependence of soil CO_2 flux based on the Q_{10} nonlinear mixed effects model. Measurements by plot and site shown, with random effect coefficients used for the best fit of plot level data (headwater wetland n = 52, upper hillslope n = 53). Black line represents the population model fit to the data (n = 525).

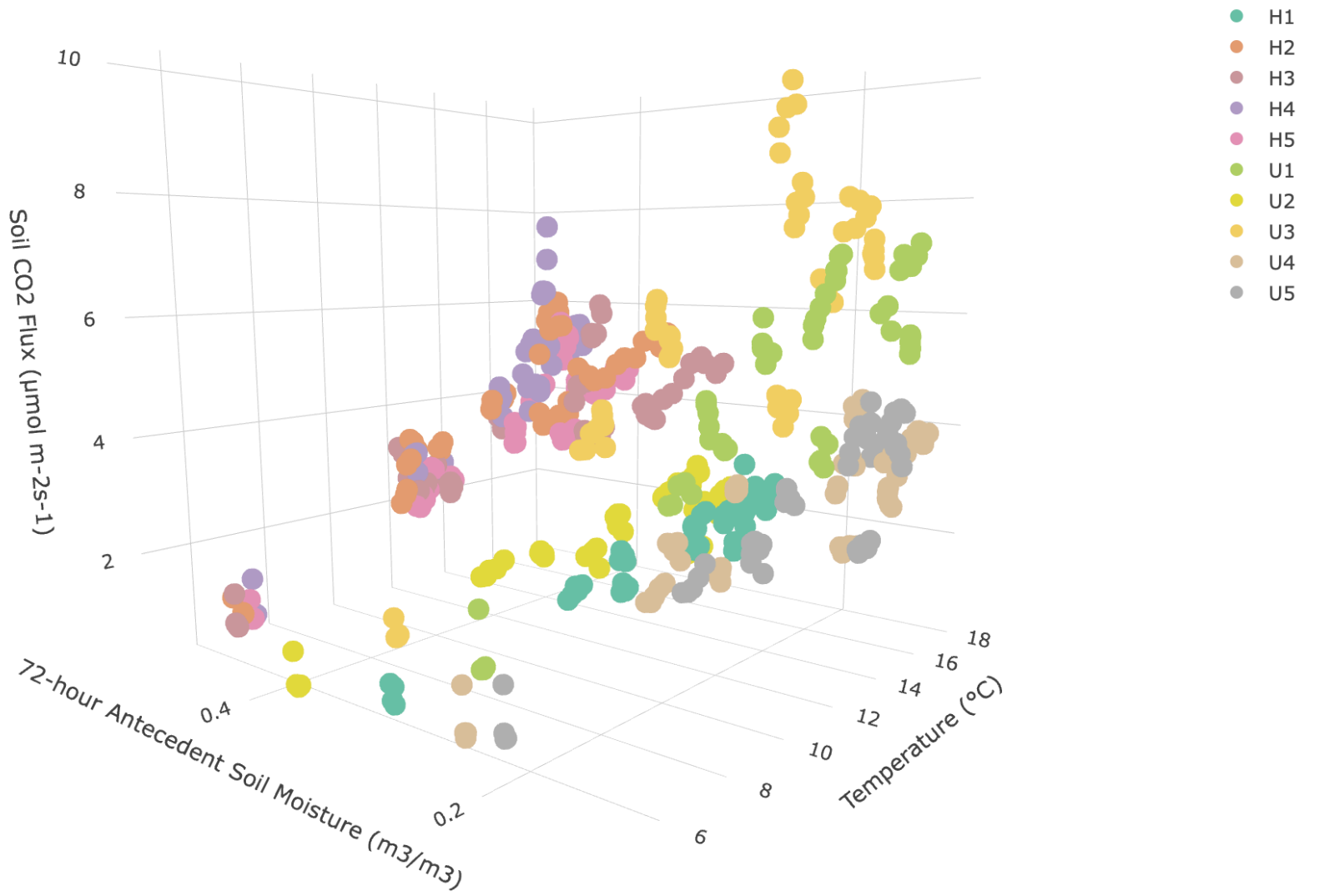

Figure 11 - Soil CO_2 flux as a function of soil temperature (°C) and 72-hour antecedent soil moisture (m^3/m^3), based on the Q_{10} and 72-hour antecedent soil moisture nonlinear mixed effects model (n = 525). Measurements shown by plot (headwater wetland n = 52, upper hillslope n = 53).

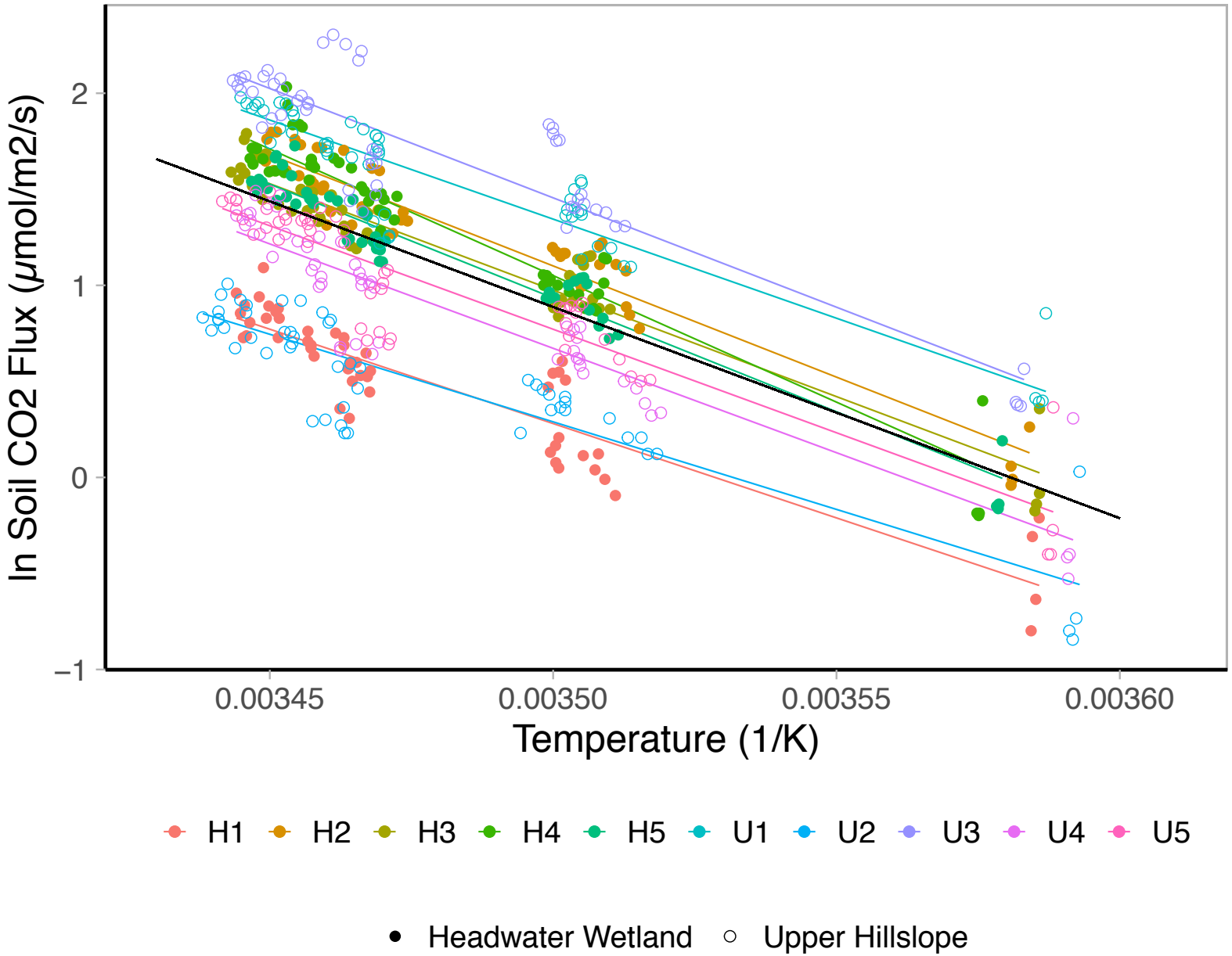

Figure 12 - Log-linear transformed temperature dependence of soil CO_2 flux based on the linear mixed effects model. Measurements shown by plot and site, with random effect coefficients used for the best fit of plot level data (headwater wetland n = 52, upper hillslope n = 53). Black line represents the population model fit for the data (n = 525).

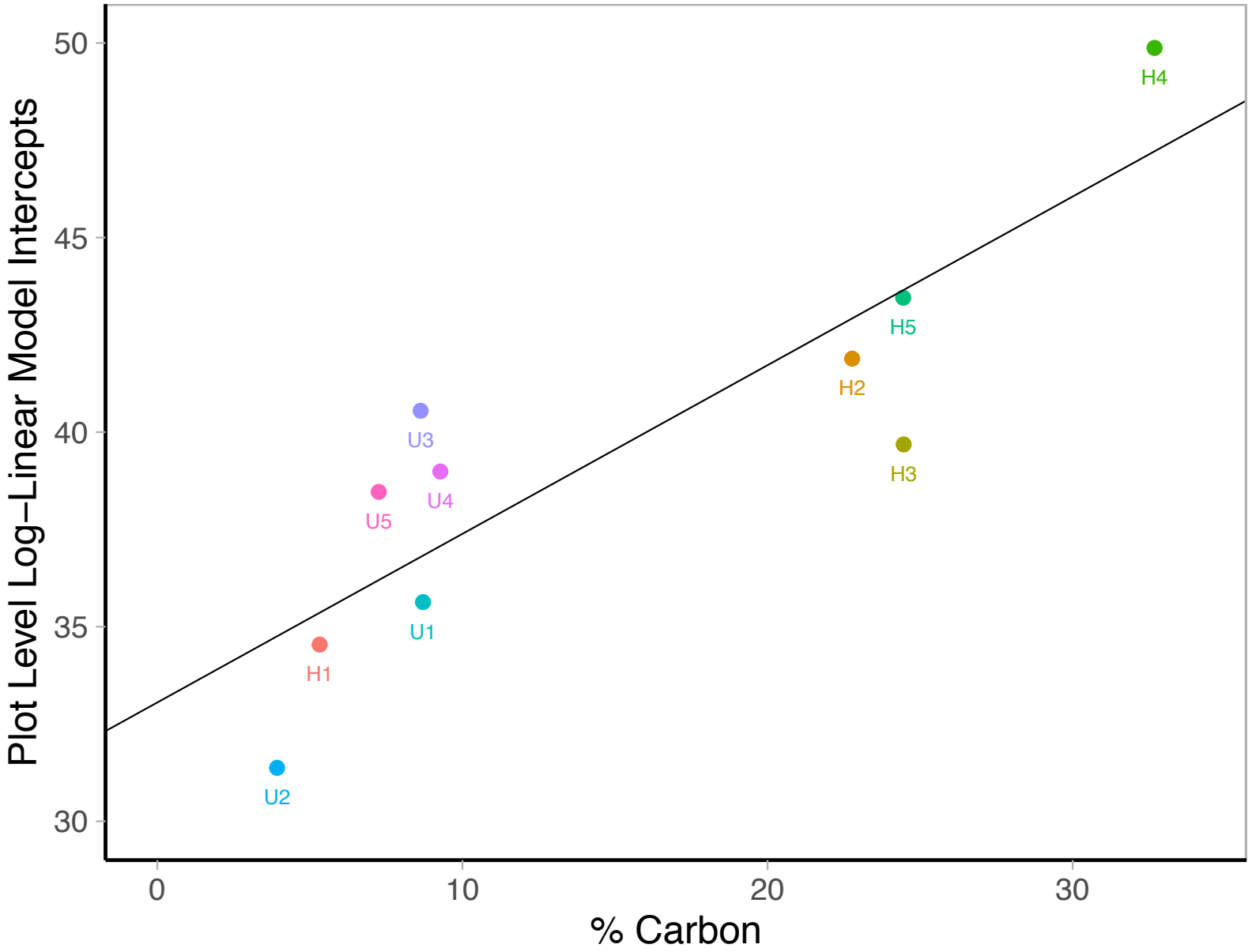

Figure 13 - Linear relationship of the plot level log-linear model intercepts and the plot level percent soil carbon content (adjusted R^2 = 0.71; n = 10).

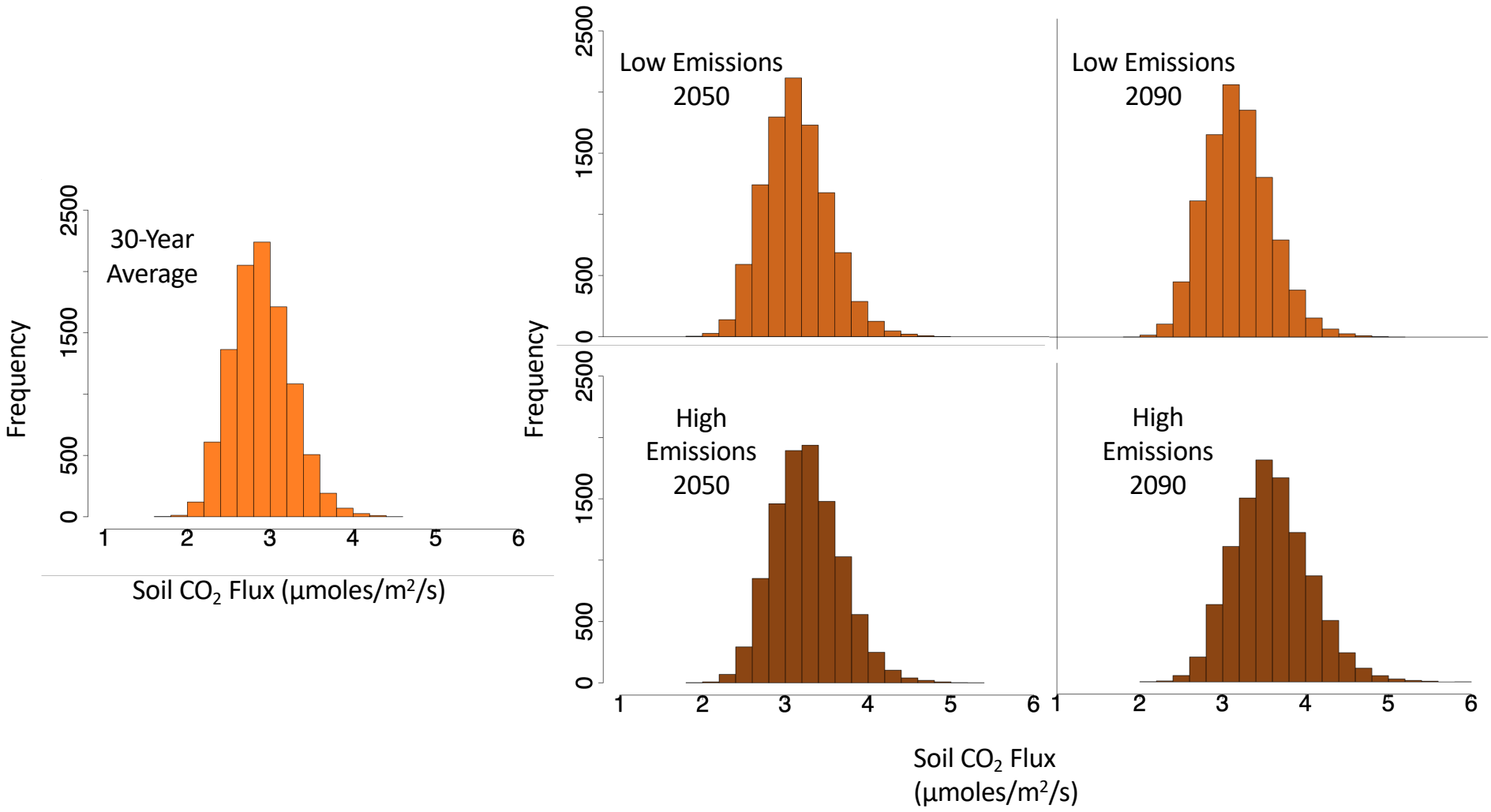

Figure 14 - Predicted soil CO_2 flux by 2050 and 2090 under two emissions scenarios. Histograms from the Monte Carlo analysis (10,000 iterations), with bootstrapping the model coefficients (intercept and slope) to account for model uncertainty, of the predicted mean soil CO_2 flux (µmoles/m^2/s) for June 1st and October 31st.

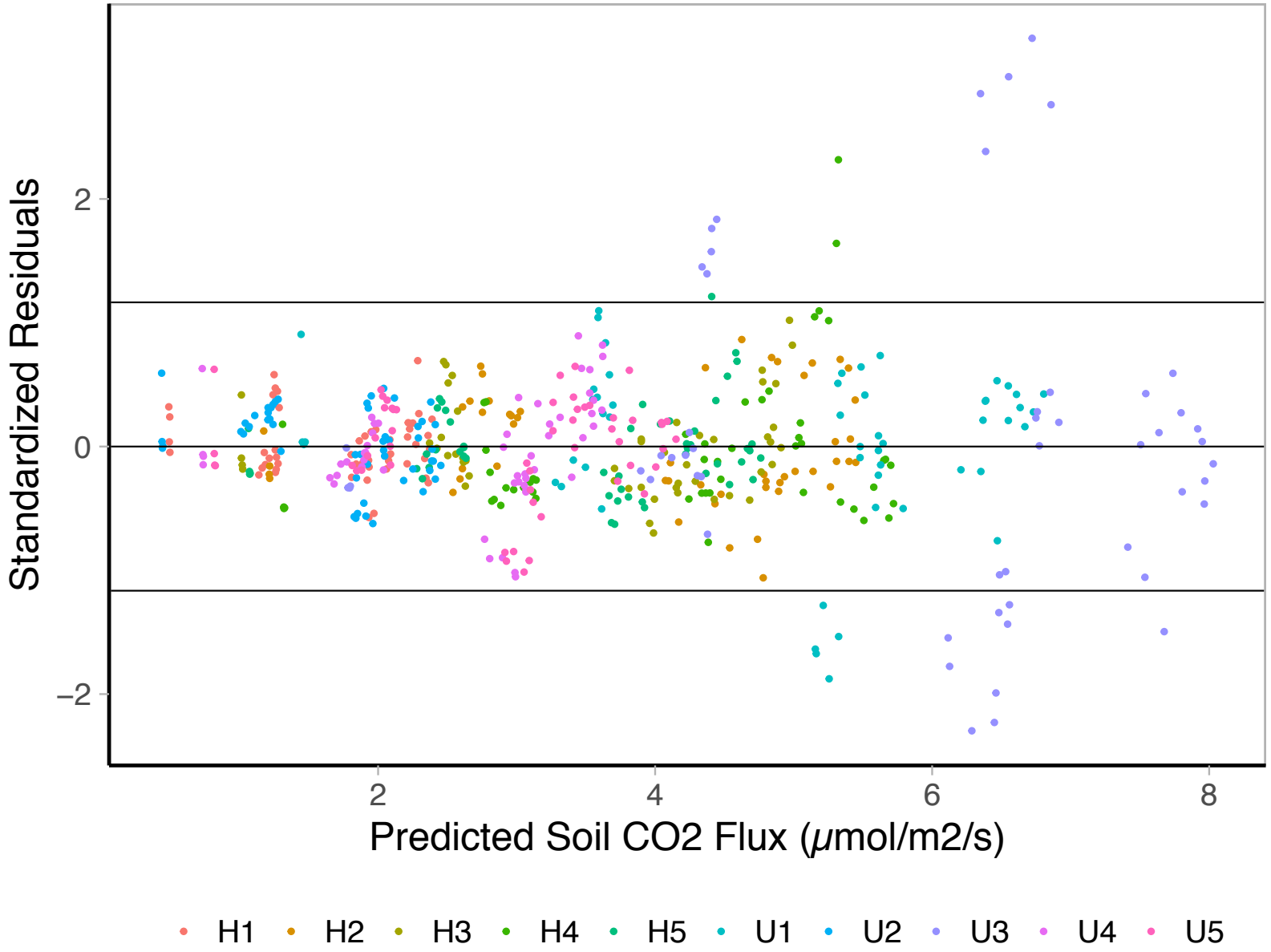

Figure 15 - Residual plot for the Q_{10} and 72-hour antecedent soil moisture nonlinear mixed effects model. Lines represent 0, 1.165, and -1.165 (2 standard deviations based on RMSE; n = 525).

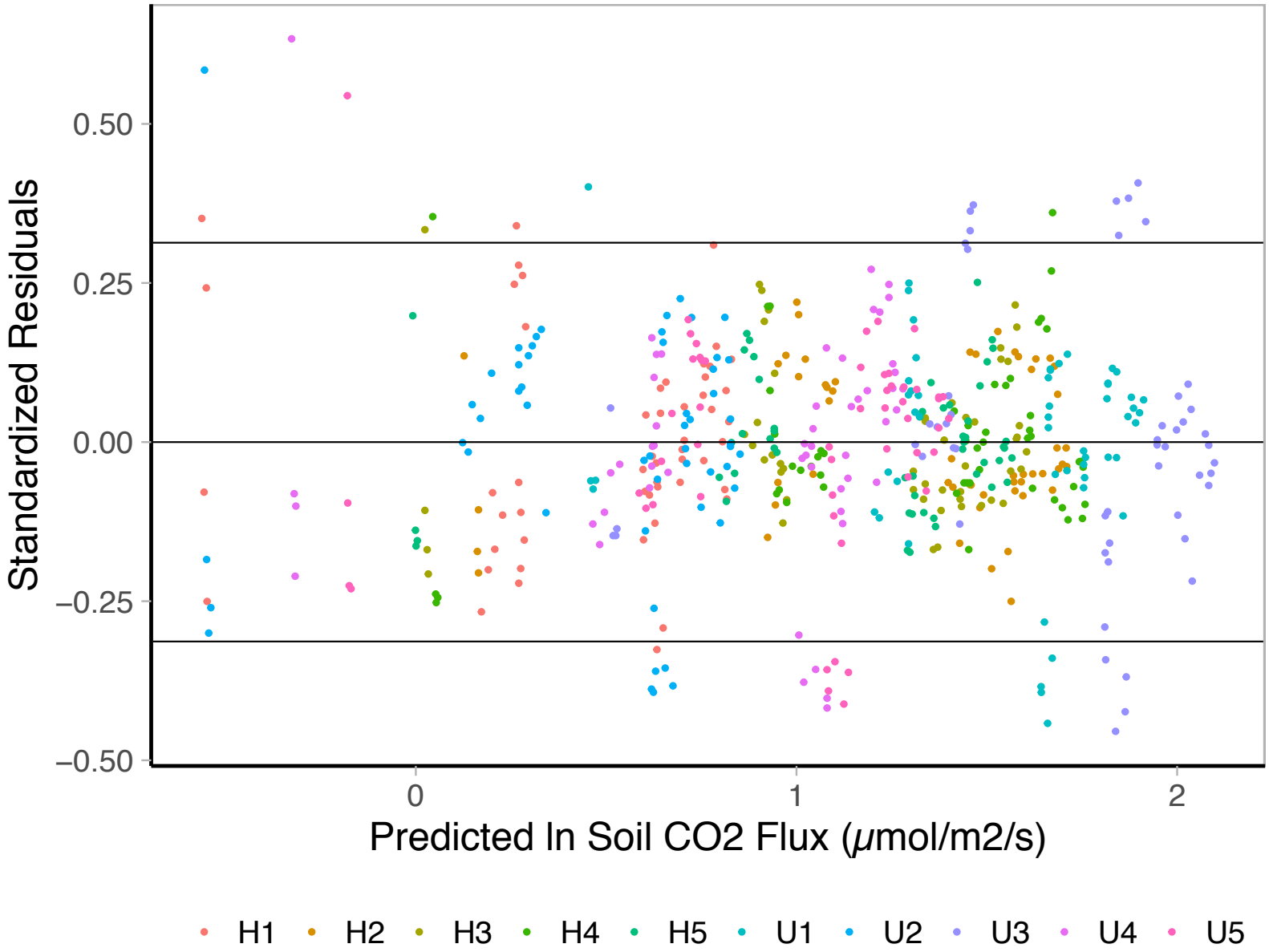

Figure 16 - Residual plot for the log-linear mixed effects model. Lines represent 0, 0.314, and -0.314 (2 standard deviations based on RMSE) (n = 525).

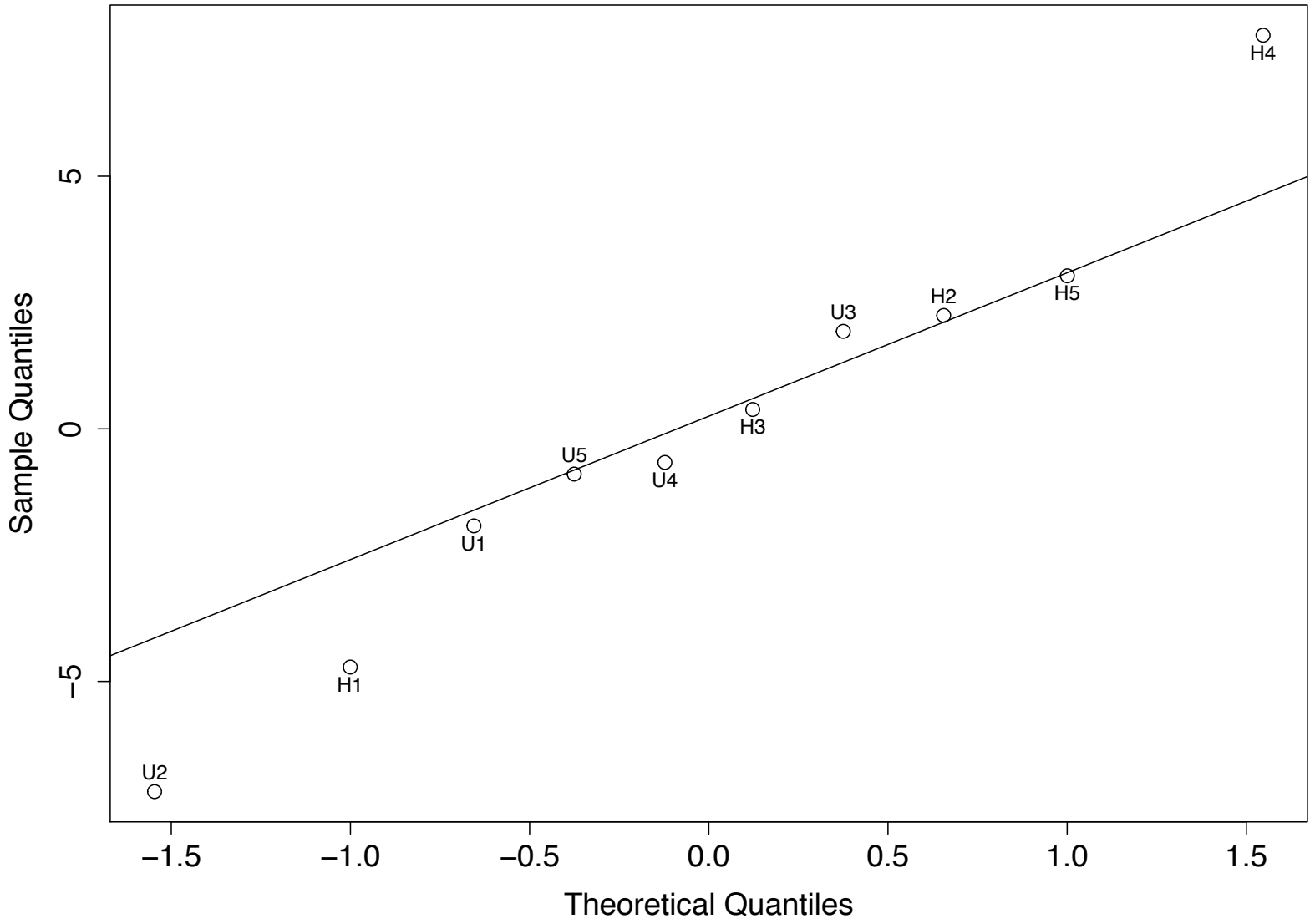

Figure 17 - Normal QQ Plot of the log-linear mixed effects model random effect of 'plot' residuals, plotted along the normal residuals line.

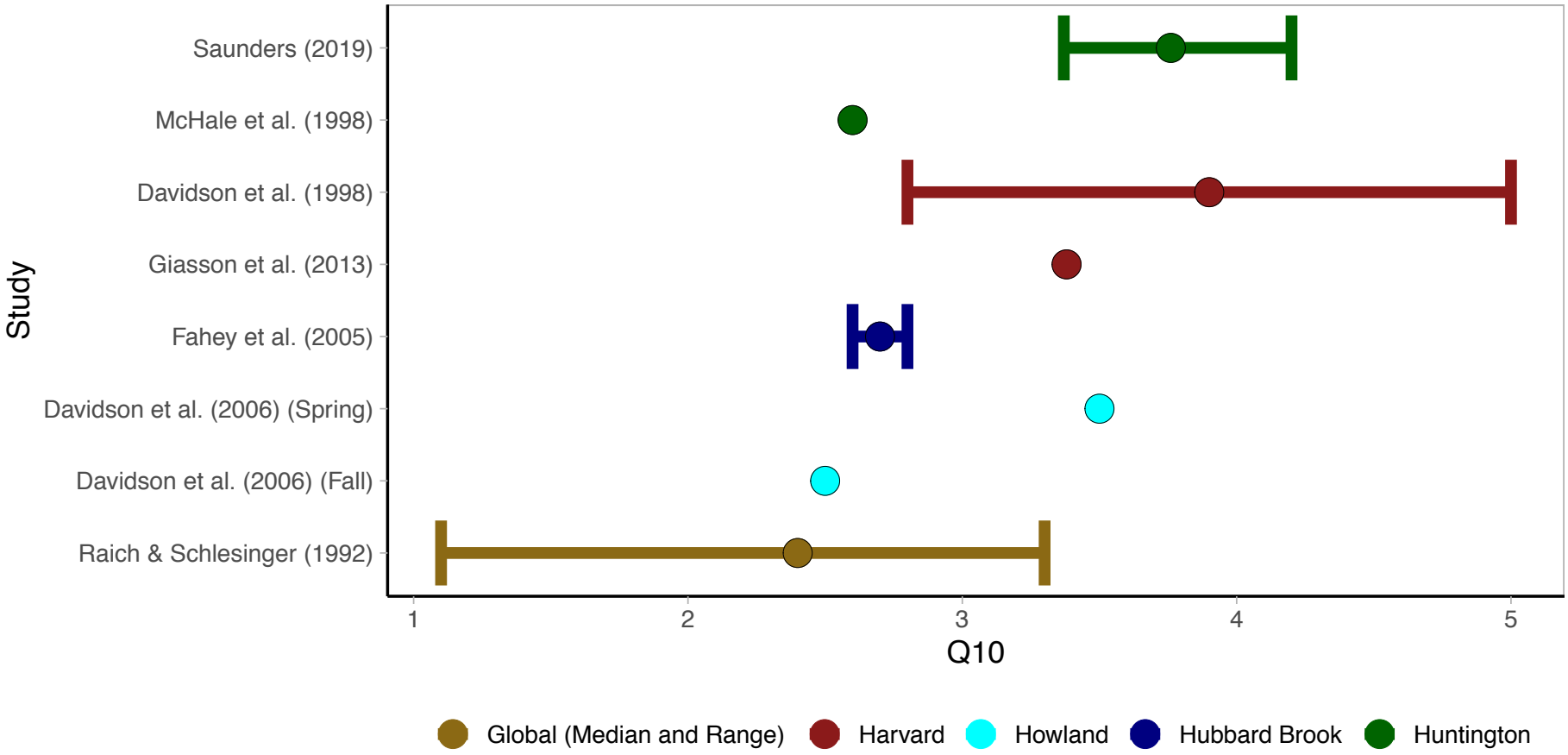

Figure 18 - Comparison of mean Q_{10} values for studies mentioned in this paper conducted in the US Northeast. Studies colored by sites, error bars represent 95% confidence interval.

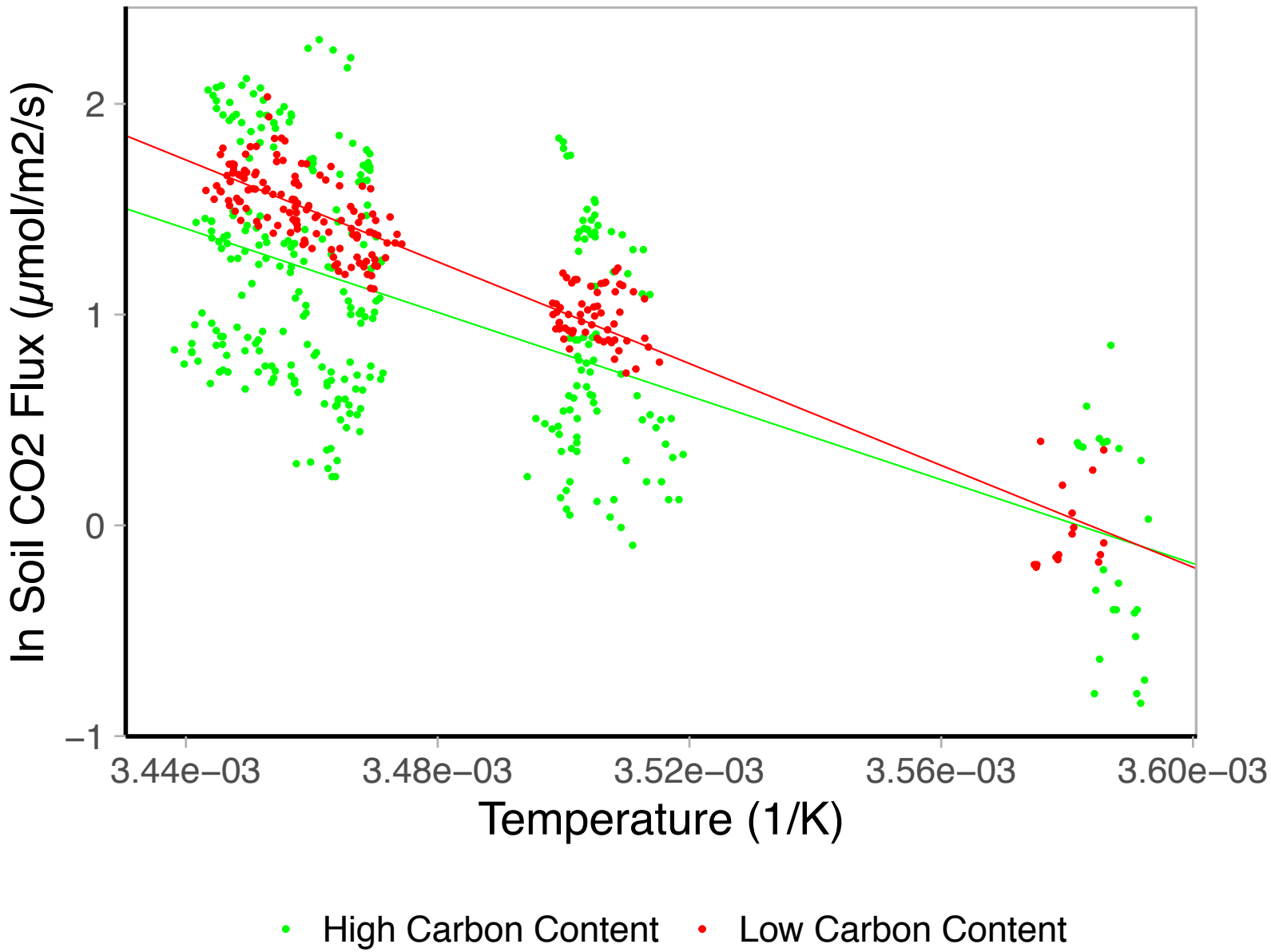

Figure 19 - Log-linear relationship between soil temperature (1/K) and the soil CO_2 flux (µmoles/m^2/s) based on carbon content in Subcatchment 14. High carbon content (n = 212) includes Plots H2, H3, H4, and H5, low carbon content (n = 318) includes plots H1, U1, U2, U3, U4, and U5.

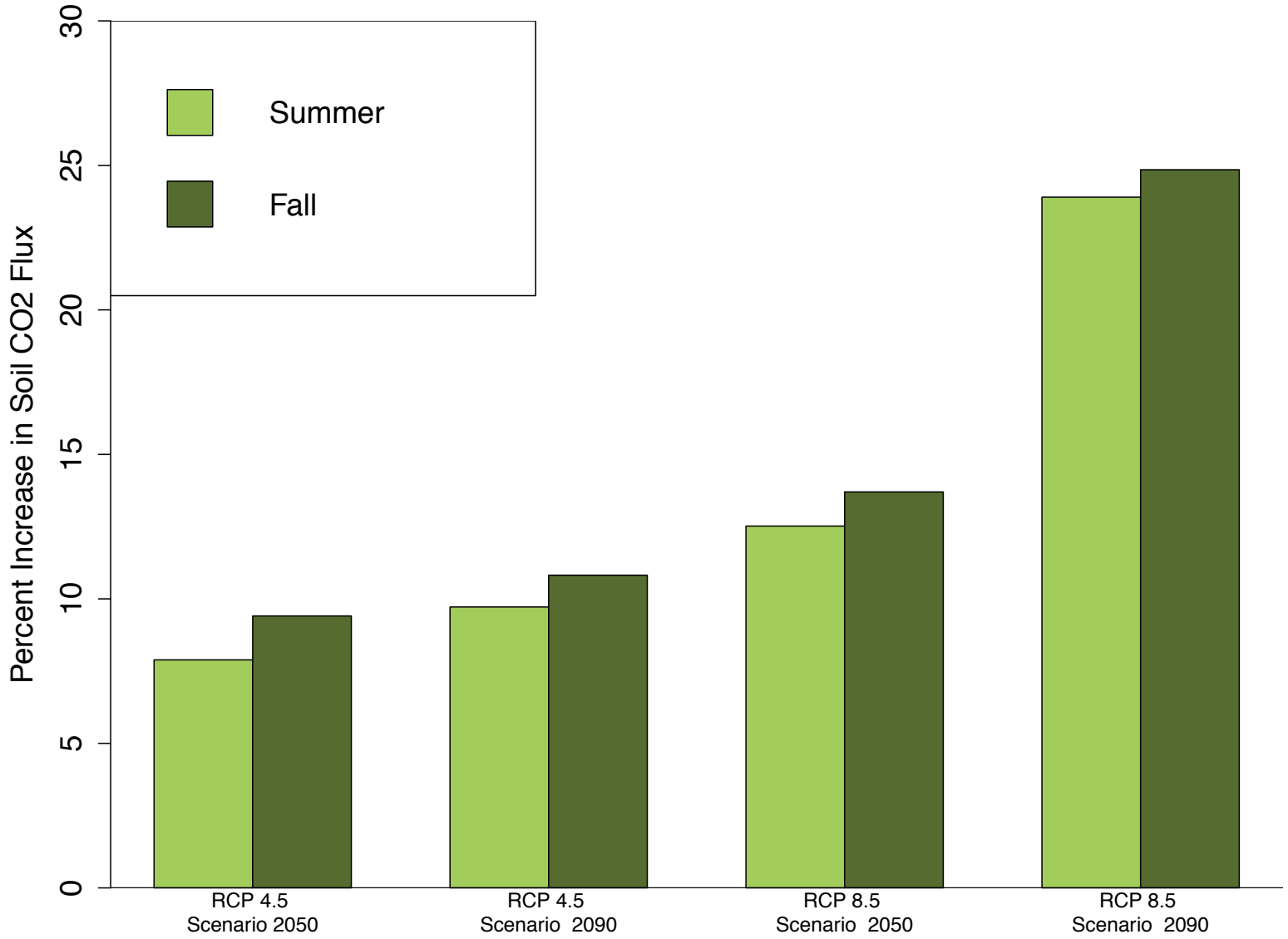

Figure 20 - Percent change in the mean soil CO_2 flux during summer (June, July, August) and fall (September, October) by 2050 and 2090 under RCP 8.5 (high emissions) and RCP 4.5 (low emissions) scenarios compared to the NWS thirty-year average predicted soil CO_2 flux. Forecasted change (Δt) for summer and fall (Table 3) were added to the thirty-year average.

Appendix A

The LI-8100A Survey System is a portable manual chamber that makes continuous flux measurements over a preset time period. Collars are inserted into the soil, where the chamber is placed on the collar, to minimize disturbance and to create an airtight seal to measure the diffusion of CO_2 from the soil surface into the chamber. The chamber keeps equal pressure with the outside ambient air through a special vent designed to minimize wind impacts, and the chambers shape allows for mixing of air. The closed system circulates air from the chamber to the IRGA and back, calculating the flux from the increasing rate of CO_2 inside the chamber. The chamber is kept sealed for a short time since the rate at which CO_2 diffuses into the chamber will change over time as the CO_2 gradient changes. A 'dead band' is preset at the beginning of the measurements to account for the mixing of the air. A line purge is done after the measurement as the chamber opens to clear the line of moisture and particles (Davidson et al., 2002; Pacaldo et al., 2014; LI-COR, 2018).

References

Akaike, H. (1978). On the Likelihood of a Time Series Model. *Journal of the Royal Statistical Society. Series D (The Statistician), 27*(3-4), 217-235. doi: 10.2307/2988185

Allison, S. D., & Treseder, K. K. (2008). Warming and drying suppress microbial activity and carbon cycling in boreal forest soils. *Global Change Biology, 14*(12), 2898-2909. doi: 10.1111/j.1365-2486.2008.01716.x

Bates D. (2007). lme4: linear mixed-effects models using S4 classes. R package, 0.99875–9. http://r-forge.r-project.org/projects/lme4/

Barr, D. J., Levy, R., Scheepers, C., & Tily, H. J. (2013). Random effects structure for confirmatory hypothesis testing: Keep it maximal. *Journal of Memory and Language*, 68(3), 255-278. doi: 10.1016/j.jml.2012.11.001

Beier, C. M., Woods, A. M., Hotopp, K. P., Gibbs, J. P., Mitchell, M. J., Dovčiak, M., et al. (2012). Changes in faunal and vegetation communities along a soil calcium gradient in northern hardwood forests. *Canadian Journal of Forest Research, 42*(6), 1141-1152. doi: 10.1139/X2012-071

Birch, H. F. (1958). The effects of soil drying on humus decomposition and nitrogen availability. *Plant and Soil, 10*(1), 9-31. doi: 10.1007/BF01343734

Brown, P. J., Bradley, R. S., Keimig, F. T. (2010). Changes in extreme climate indices for the Northeastern United States, 1870–2005. *Journal of Climate, 23*(24), 6555-6572. doi: 10.1175/2010JCLI3363.1

Burnham, K. P., & Anderson, D. R. (2004). Multimodel Inference: Understanding AIC and BIC in Model Selection. *Sociological Methods Research, 33*(2), 261-304. doi: 10.1177/0049124104268644

Carey, J. C., Tang, J., Templer, P. H., Kroeger, K. D., Crowther, T. W., Burton, A. J., et al. (2016). Temperature response of soil respiration largely unaltered with experimental warming. *Proceedings of the National Academy of Sciences of the United States of America, 113*(48), 13797-13802. doi: 10.1073/pnas.1605365113

Chen, J., Franklin, J. F. & Spies, T. A. (1993). Contrasting microclimates among clearcut, edge, and interior of old-growth Douglas-fir forest. *Agricultural and Forest Meteorology, 63*(3-4), 219-237. doi: 10.1016/0168-1923(93)90061-L

Christopher, S.F., Page, B. D., Campbell, J. L., & Mitchell, M. J. (2006). Contrasting stream water NO^-_3 and Ca^{2+} in two nearly adjacent catchments: the role of soil Ca and forest vegetation. *Global Change Biology, 12*(2)*,* 364-381. doi: 10.1111/j.1365-2486.2005.01084.x

Davidson, E. A., Belk, E., & Boone, R. D. (1998). Soil water content and temperature as independent or confounded factors controlling soil respiration in a temperate mixed hardwood forest. *Global Change Biology, 4*(2), 217-227. doi: 10.1046/j.1365-2486.1998.00128.x

Davidson, E. A., Verchot, L. V., CattânioI, J. H., Ackerman, I. L., & Carvalho, J. E. M. (2000). Effects of soil water content on soil respiration in forests and cattle pastures of eastern Amazonia. *Biogeochemistry, 48*(1), 55-69. doi: 10.1023/A:1006204113917

Davidson, E. A., Savage, K., Verchot, L. V., & Navarro, R. (2002). Minimizing artifacts and biases in chamber-based measurements of soil respiration. *Agricultural and Forest Meteorology, 113*(1-4), 21-37. doi: 10.1016/S0168-1923(02)00100-4

Davidson, E. A. & Janssens, I. A. (2006). Temperature Sensitivity of Soil Carbon Decomposition and Feedbacks to Climate Change. *Nature, 440*(7081), 165-173. doi: 10.1038/nature04514

Davidson, E. A., Janssens, I. A., & Luo, Y. (2006). On the variability of respiration in terrestrial ecosystems: moving beyond Q_{10}. *Global Change Biology, 12*(2), 154-164. doi: 10.1111/j.1365-2486.2005.01065.x

Davidson, E. A, & Janssens, I. A (2006). Temperature sensitivity of soil carbon decomposition and feedbacks to climate change. *Nature, 440*(7081), 165-173. doi: 10.1038/nature04514

Davidson, E. A., Samanta, S., Caramori, S. S., & Savage, K. (2012). The Dual Arrhenius and Michaelis-Menten kinetics model for decomposition of soil organic matter at hourly to seasonal time scales. *Global Change Biology, 18*(1), 371-384. doi: 10.1111/j.1365-2486.2011.02546.x

DeGaetano, A. T. (2009). Time-dependent changes in extreme-precipitation return-period amounts in the continental United States. *Journal of Applied Meteorology and Climatology, 48*(10), 2086-2099. doi: 10.1175/2009JAMC2179.1

de Freitas, C. R., & Enright, N. J. (1995). Microclimatic differences between and within canopy gaps in a temperate rainforest. *International Journal of Biometeorology, 38*(4), 188-193. doi: 10.1007/BF01245387

Diffenbaugh, N. S., Scherer, M., & Trapp, R. J. (2013). Robust increases in severe thunderstorm environments in response to greenhouse forcing. *Proceedings of the National Academy of Sciences of the United States of America, 110*(41), 16361-16366. doi: 10.1073/pnas.1307758110

Fahey, T. J., Tierney, G. L., Fitzhugh, R. D., Wilson, G. F., & Siccama, T. G. (2005). Soil respiration and soil carbon balance in a northern hardwood forest ecosystem. *Canadian Journal of Forest Research, 35*(2), 244-253. doi: 10.1139/x04-182

Fetcher, N., Oberbauer, S. F. & Strain, B. R. (1985). Vegetation effects on microclimate in lowland tropical forest in Costa Rica. *International Journal of Biometeorology, 29*(2), 145-155. doi: 10.1007/BF02189035

Giasson, M. -A., Ellison, A. M., Bowden, R. D., Crill, P. M., Davidson, E. A., Drake, J. E., et al. (2013). Soil respiration in a Northeastern US temperate forest: a 22-year synthesis. *Ecosphere, 4*(11), 1-28. doi: 10.1890/ES13.00183.1

Gomez, J. (2014). Soil-atmosphere carbon dioxide, methane, and nitrous oxide fluxes across time and space in a forested watershed. Master's Thesis, State University of New York, College of Environmental Science and Forestry, 2014.

Griffiths, M. L., & Bradley, R. S. (2007). Variations of twentieth-century temperature and precipitation extreme indicators in the Northeast United States. *Journal of Climate, 20*(21), 5401-5417. doi: 10.1175/2007JCLI1594.1

Groffman, P. M., Driscoll, C. T., Fahey, T. J., Hardy, J. P., Fitzhugh, R. D., & Tierney, G. L. (2001). Colder soils in a warmer world: a snow manipulation study in a northern hardwood forest ecosystem. *Biogeochemistry, 56*(2), 135-150. doi: 10.1023/A:1013039830323

Gross, J. M. (2012). Hydrogeomorphology and antecedent moisture condition controls on greenhouse gas dynamics in forested landscapes of the US Northeast. Master's Thesis, State University of New York, College of Environmental Science and Forestry, 2012.

Harper, C. W., Blair, J. M., Fay, P. A., Knapp, A. K., & Carlisle, J. D. (2005). Increased rainfall variability and reduced rainfall amount decreases soil CO_2 flux in a grassland ecosystem. *Global Change Biology, 11*(2), 322-334. doi: 10.1111/j.1365-2486.2005.00899.x

Harper, K. A., MacDonald, S. E., Burton, P. J., Chen, J., Brosofske, K. D., Saunders, S. C. et al. (2005). Edge influence on forest structure and composition in fragmented landscapes. *Conservation Biology, 19*(3), 768-782. doi: 10.1111/j.1523-1739.2005.00045.x

Harrison, X. A., Donaldson, L., Correa-Cano, M. E., Evans, J., Fisher, D. N., Goodwin, C. E. D., et al. (2018). A brief introduction to mixed effects modelling and multi-model inference in ecology. *PeerJ, 6*, e4794. doi:10.7717/peerj.4794

Homan, C., Beier, C., McCay, T., & Lawrence, G. (2016). Application of lime (CaCO3) to promote forest recovery from severe acidification increases potential for earthworm invasion. *Forest Ecology and Management, 368*(15), 39-44. doi: 10.1016/j.foreco.2016.03.002

Horton, R., Bader, D., Tryhorn, L., DeGaetano, A., & Rosenzweig, C. (2014). Climate Risks. In New York State Energy Research and Development Authority (NYSERDA) (Ed.), *Responding to climate change in New York State: The ClimAID integrated assessment for effective climate change adaptation in New York State* (pp. 15-48). Retrieved from https://www.nyserda.ny.gov

Howarth, M.E., C.D. Thorncroft, & L. F. Bosart, 2019: Changes in Extreme Precipitation in the Northeast United States: 1979–2014. J. *Hydrometeor*., 0, https://doi.org/10.1175/JHM-D-18-0155.1

Insaf, T. Z., Lin, S., & Sheridan, S. C. (2012). Climate trends in indices for temperature and precipitation across New York State, 1948–2008. *Air Quality, Atmosphere & Health, 6*(1), 247-257. doi: 10.1007/s11869-011-0168-x

Knapp, A. K., Fay, P. A., Blair, J. M., Collins, S. L., Smith, M. D., Carlisle, J. D., et al. (2002). Rainfall variability, carbon cycling, and plant species diversity in a mesic grassland. *Science, 298*(5601), 2202-2205. doi: 10.1126/science.1076347

Lee, M-S., Nakane, K., Nakatsubo, T., Mo, W-H., & Koizumi, H. (2002). Effects of rainfall events on soil CO_2 flux in a cool temperate deciduous broad-leaved forest. *Ecological Research, 17*(3)*,* 401-409. doi: 10.1046/j.1440-1703.2002.00498.x

LI-COR (2018). *Soil Gas Flux.* Retrieved on May 14, 2018 from https://www.licor.com/env/products/soil_flux/

Liang, N., Nakadai, T., Hirano, T., Qu, L., Koike, T., Fujinuma, Y., et al. (2004). In-situ comparison of four approaches to estimating soil CO_2 efflux in a northern larch (Larix kaempferi Sarg.) forest. *Agricultural and Forest Meteorology, 123*(1-2), 97-117. doi: 10.1016/j.agrformet.2003.10.002

Lloyd, J., & Taylor, J. A. (1994). On the temperature dependence of soil respiration. *Functional Ecology, 8*(3), 315-323. doi: 10.2307/2389824

Maxim Integrated. (2018). iButton Temperature Loggers. Retrieved on May 4, 2018 from https://www.maximintegrated.com/en/products/ibutton/data-loggers/DS1922L.html

McHale, P. J., Mitchell, M. J., & Bowles, F. P. (1998). Soil warming in a northern hardwood forest: trace gas fluxes and leaf litter decomposition. *Canadian Journal of Forest Research. 28*(9), 1365-1372. doi: 10.1139/x98-118

METER Group (2018). *ECH2O GS 1, ECH2O Em50.* Retrieved on May 4, 2018 from https://www.metergroup.com/environment/products/ech2o-gs-1/

The National Aeronautics and Space Administration (NASA). (2019). [Map of the GRACE Surface Soil Moisture, Root Zone Soil Moisture, and Ground Water Percentile of weekly data]. *NASA Grace Map Archive.* Retrieved on March 27, 2019 from https://nasagrace.unl.edu/Archive.aspx

The National Drought Mitigation Center, University of Nebraska-Lincoln (NDMC). (2019a) *United States Drought Monitor – Drought Summary.* Retrieved on March 27, 2019 from https://droughtmonitor.unl.edu/ DroughtSummary.aspx

The National Drought Mitigation Center, University of Nebraska-Lincoln (NDMC). (2019b) [Map of the US Drought Monitor New York state drought conditions weekly data]. *United States Drought Monitor – Map Archives.* Retrieved on March 20, 2019 from https://droughtmonitor.unl.edu/Maps/MapArchive.aspx

The National Oceanic and Atmospheric Administration (NOAA). (2019). [Map of the Weekly Palmer Drought Indices in the United States]. *Weekly Palmer Drought Indices.* Retrieved on March 27, 2019 from https://www.ncdc.noaa.gov/temp-and-precip/drought/weekly-palmers/20180901

The National Weather Service (NWS) (2018). *Burlington, Vermont Local Climate Data and Plots.* [Data set]. Retrieved on March 20, 2018, available from https://w2.weather.gov/climate/xmacis.php?wfo=btv

The National Weather Service (NWS) (2019). [Map of the monthly Soil Moisture and Temperature anomalies and percentile in the United States]. *Land Surface Monitoring and Prediction CPC Leaky Bucket Model.* Retrieved on April 1, 2019 from https://www.cpc.ncep.noaa.gov/products/Soilmst_Monitoring/index.shtml

The New York Climate Change Mapping Tool. (2019). [interactively map of data a related to climate change impacts, vulnerability and adaptation across New York]. Retrieved on April 10, 2018, available from http://nymapnescaumccscdataservices.s3websiteuseast1.amazonaws.com/?map_state_token=825a51ea2d9bad0c384ed43973f042f8

New York State Mesonet. (2018). *New York State's Mesoscale Weather Network.* [Data set]. Retrieved on March 20, 2018, available from http://www.nysmesonet.org/

Pacaldo, R. S., Volk, T. A, Briggs, R. D., Abrahamson, L. P., Bevilacqua, E., & Fabio, E. S. (2014). Soil CO_2 effluxes, temporal and spatial variations, and root respiration in shrub willow biomass crops fields along a 19-year chronosequence as affected by regrowth and removal treatments. *Global Change Biology Bioenergy, 6*(5), 488-498. doi: 10.1111/gcbb.12108

Pierce, D. W., Cayan, D. R., & Thrasher, B. L. (2014). Statistical Downscaling Using Localized Constructed Analogs (LOCA). *Journal of Hydrometeorology, 15*(6), 2558-2585. doi: 10.1175/JHM-D-14-0082.1

R Development Core Team. (2019) R: a language and environment for statistical computing. Vienna (Austria). R Foundation for Statistical Computing

Raftery, A. E., Madigan, D., & Hoeting, J. A. (1993). Model selection and accounting for model uncertainty in linear regression models. Technical Report no 262, Department of Statistics, University of Washington

Raich, J. W., & Schlesinger, W. H. (1992). The global carbon dioxide flux in soil respiration and its relationship to vegetation and climate. *Tellus, 44*(2), 81-99. doi: 10.1034/j.1600-0889.1992.t01-1-00001.x

Raich, J. W., Potter, C. S., & Bhagawati, D. (2002). Interannual variability in global soil respiration, 1980–94. *Global Change Biology, 8*(8), 800-812. doi: 10.1046/j.1365-2486.2002.00511.x

Richey, D. G. (1994). Nitrous oxide, methane and carbon dioxide flux between forest soils and the atmosphere and the effects of ammonium sulfate fertilization. Master's Thesis, Syracuse University, 1994. C. Driscoll, Personal Communication, December 7, 2017.

Ryan, M. G., & Law, B. E. (2005). Interpreting, measuring, and modeling soil respiration. *Biogeochemistry, 73*(1), 3-27. doi: 10.1007/s10533-004-5167-7

Savage, K. E., & Davidson, E. A. (2001). Interannual variation of soil respiration in two New England forests. *Global Biogeochemical Cycles, 15*(2), 337-350. doi: 10.1029/1999GB001248

Schielzeth, H., & Forstmeier, W. (2009). Conclusions beyond support: overconfident estimates in mixed models. *Behavioral Ecology, 20*(2), 416-420. doi: 10.1093/beheco/arn145

Schipper, L. A., Hobbs, J. K., Rutledge, S. & Arcus, V. L. (2014). Thermodynamic theory explains the temperature optima of soil microbial processes and high Q10 values at low temperatures. *Global Change Biology, 20*(11), 3578-3586. doi: 10.1111/gcb.12596

Schlesinger, W. H., & Andrews, J. A. (2000). Soil respiration and the global carbon cycle. *Biogeochemistry, 48*(1), 7-20. doi: 10.1023/A:1006247623877

Senevirante, S. I., Corti, T., Davin, E. L., Hirschi, M., Jaeger, E. B., Lehner, I., et al. (2010). Investigating soil moisture–climate interactions in a changing climate: a review. *Earth-Science Reviews, 99*(3-4), 125-161. doi: 10.1016/j.earscirev.2010.02.004

Sillmann, J., Kharin, V. V., Zwiers, F. W., Zhang, X., & Bronaugh, D. (2013). Climate extremes indices in the CMIP5 multimodel ensemble: Part 2. Future climate projections. *JGR Atmospheres, 118*(6), 2473-2493. doi: 10.1002/jgrd.50188

Singh, D., Tsiang, M., Rajaratnam, B., & Diffenbaugh, N. (2013). Precipitation extremes over the continental United States in a transient, high-resolution, ensemble climate model experiment. *Journal of Geophysical Research: Atmospheres, 118*(13), 7063-7086. doi: 10.1002/jgrd.50543

Somers Jr., R. C. (1986). Soil classification, genesis, morphology and variability of soils found within the Central Adirondack Region of New York. Doctoral dissertation, State University of New York, College of Environmental Science and Forestry, 1986.

State University of New York, College of Environmental Science and Forestry (SUNY ESF). (2018). Environmental Monitoring. Retrieved on May 18, 2018 from https://www.esf.edu/hss/em/index.html

Strong, T. F., Teclaw, R. M., & Zasada, J.C. (1997). Monitoring the effects of partial cutting and gap size on microclimate and vegetation responses in northern hardwood forests in Wisconsin. In United States Department of Agriculture Forest Service (Ed.), *Communicating the Role of Silviculture in Managing the National Forests, Proceedings of the National Silviculture Workshop* (pp. 42-47). Retrieved from https://www.nrs.fs.fed.us/pubs/gtr/gtr_ne238/gtr_ne238.pdf

Thibeault, J. M., Seth, A. (2014) Changing climate extremes in the Northeast United States: observations and projections from CMIP5. *Climatic Change, 127*(2), 273-287. doi: 10.1007/s10584-014-1257-2

Ullah, S., & Moore, T. R. (2011). Biogeochemical controls on methane, nitrous oxide, and carbon dioxide fluxes from deciduous forest soils in eastern Canada. *Journal of Geophysical Research Biogeosciences, 116*(G3), 1-15 doi: 10.1029/2010JG001525

U.S. Global Change Research Program (USGCRP) (2018). *National Climate Assessment.* Retrieved on November 4, 2019 from https://nca2018.globalchange.gov/

Vrugt, J. A., Gupta, H. V., Bouten, W., & Sorooshian, S. (2003). A Shuffled Complex Evolution Metropolis algorithm for optimization and uncertainty assessment of hydrologic model parameters. *Water Resources Research, 39*(8), 1-1 - 1-14. doi: 10.1029/2002WR001642

Warren, C. R. (2014). Do microbial osmolytes or extracellular depolymerisation products accumulate as soil dries? *Soil Biology and Biochemistry, 98*, 54-63. doi: 10.1016/j.soilbio.2016.03.021

Warren, C. R. (2016). Response of osmolytes in soil to drying and rewetting. *Soil Biology and Biochemistry, 70*, 22-32. doi: 10.1016/j.soilbio.2013.12.008

Wilby, R. L. (2005). Uncertainty in water resource model parameters used for climate change impact assessment. *Hydrological Processes, 19(16)*, 3201-3219. doi: 10.1002/hyp.5819

Winter, B. (2013). Linear models and linear mixed effects models in R with linguistic applications. arXiv:1308.5499. [http://arxiv.org/pdf/1308.5499.pdf]

Wuebbles, D. J., Kunkel, K., Wehner, M., & Zobel, Z. (2014). Severe weather in United States under a changing climate. EOS, Transactions, American Geophysical Union, (95)18, 149-150. doi: 0.1002/2014EO180001

Xu, L., Baldocchi, D. D., & Tanh, J. (2004). How soil moisture, rain pulses, and growth alter the response of ecosystem respiration to temperature. *Global Biogeochemical Cycle, 18*(4), 1-10. doi: 10.1029/2004GB002281

Yuste, J. C., Janssens, I. A., Carrara, A., Meiresonne, L., & Ceulemans, R. (2003). Interactive effects of temperature and precipitation on soil respiration in a temperate maritime pine forest. *Tree Physiology, (23)*18, 1263-1270. doi: 10.1093/treephys/23.18.1263

Zaragoza-Castells, J., Sánchez-Gómez, D., Hartley, I. P., Matesanz, S., Valladares, F., Lloyd, J. et al. (2008). Climate-dependent variations in leaf respiration in a dry-land, low productivity Mediterranean forest: the importance of acclimation in both high-light and shaded habitats. *Functional Ecology, 22*(1), 172-184. doi: 10.1111/j.1365-2435.2007.01355.x

Resume

Will Saunders

23 Water St Apt 1 | Baldwinsville NY, 13027 | 732-546-8740 | willib48@gmail.com

EDUCATION

State University of New York College of Environmental Science and Forestry December 2019

Master of Science, Forest Resources Management Syracuse, NY

- Thesis: Fine-scale microclimatic controls of soil carbon dioxide fluxes in a northern hardwood forest

The University of Maine May 2013

Bachelor of Science, Ecology and Environmental Science, Economics Minor Orono, ME

- Thesis: Vulnerability of the South Pacific to climate change due to globalization
- Group Thesis: Local economic impacts of the proposed Maine East-West Highway

PROFESSIONAL EXPERIENCE

State University of New York College of Environmental Science and Forestry August 2017 - present

Research Assistant Syracuse, NY

- Instructed students, and conducted data collection and analysis as part of Dr. Colin Beier's Forest Ecosystems Lab
- Fabrication, deployment and analysis of temperature and soil moisture arrays in the Adirondack State Park
- Soil respiration and carbon dioxide flux analysis using a dynamic chamber and infrared gas analyzer

Cardno May 2014 - present

Ecological Restoration Project Manager Syracuse, NY

- Conducted native wetland planting, stream bank stabilization, invasive species control, Phase I / II archeology, etc.
- Procured materials, prepared quotes, plans, reports and correspondence to meet client specifications and deadlines
- Project management and crew supervision for Onondaga Lake Habitat Restoration project during 2015-2017
- Contributed on projects in New York, Michigan and Indiana, including Hudson River Dredging Project, Buffalo River Restoration Project, Dakota Access Pipeline Project and Illiana Corridor Project

E&S Environmental Chemistry, Inc. April – June 2019

Database and Data Analyst Syracuse, NY

- Performed literature review towards the creation of a Greenhouse Gas budget for New York State Energy Research and Development Authority (NYSERDA)

Fund for the Public Interest May – August 2012

Field Manager for Environment New Jersey New Brunswick, NJ

- Managed canvassing crews campaigning for the clean-up of Barnegat Bay
- Corresponded with state representatives and media on local environmental issues
- Recommended for Assistant Director position in local field office